PHOTOVOLTAIC AND THERMAL SYSTEM APPLICATIONS WITH DIFFERENT TYPE FLUIDS

2021
PhD THESIS
DEPARTMENT OF ENERGY SYSTEMS ENGINEERING

Ismail ALBARKI

Thesis Advisor
Prof Dr. Ilhan CEYLAN

PHOTOVOLTAIC AND THERMAL SYSTEMS APPLICATIONS WITH DIFFERENT TYPE FLUIDS

Ismail ALBARKI

T.C.
Karabuk University
Institute of Graduate Programs
Department of Energy Systems Engineering
Prepared as
PhD Thesis

Thesis Advisor
Prof. Dr. Ilhan CEYLAN

KARABUK
June 2021

I certify that in my opinion the thesis submitted by Ismail ALBARKI titled "PHOTOVOLTAIC AND THERMAL SYSTEM APPLICATIONS WITH DIFFERENT TYPE FLUIDS" is fully adequate in scope and in quality as a thesis for the degree of PhD.

Prof. Dr. Ilhan CEYLAN .....
Thesis Advisor, Department of Energy Systems Engineering

This thesis is accepted by the examining committee with a unanimous vote in the Department of Energy Systems Engineering as a PhD thesis. June 25, 2021

Examining Committee Members (Institutions)	Signature
Chairman : Prof. Dr. Sezayi YILMAZ (KBU)	.....
Member : Prof. Dr. İlhan CEYLAN (KBU)	.....
Member : Assoc. Prof. Dr. Ali Etem GUREL (DU)	.....
Member : Assoc. Prof. Dr. Volkan KIRMACI (BU)	.....
Member : Assist. Prof. Dr. Ali CAN (KBU)	.....

The degree of PhD by the thesis submitted is approved by the Administrative Board of the Institute of Graduate Programs, Karabuk University.

Prof. Dr. Hasan SOLMAZ .....
Director of the Institute of Graduate Programs

“I declare that all the information within this thesis has been gathered and presented in accordance with academic regulations and ethical principles and I have according to the requirements of these regulations and principles cited all those which do not originate in this work as well.”

Ismail ALBARKI

ABSTRACT

Ph. D. Thesis

PHOTOVOLTAIC AND THERMAL SYSTEMS APPLICATIONS WITH DIFFERENT TYPE FLUIDS

Ismail ALBARKI

Karabuk University
Institute of Graduate Programs
Department of Energy Systems Engineering

Thesis advisor:
Prof. Dr. İlhan CEYLAN
June 2021, 98 pages

Decreasing the temperature of photovoltaic modules increases the power obtained from the module and the module efficiency. In this study, a new application has been tried to increase the efficiency of PV modules. Air or liquid fluids can be used as refrigerants in PV modules.

The reuse of the refrigerant used in the modules in the system is important in terms of energy balance and savings. In this study, PV modules were cooled using different fluids by means of spiral pipes placed behind the module. The liquid fluid heated during the cooling of the PV modules was evaluated in the same system for heating the air used for heating in the winter season. As a result of the experiments carried out during the winter months, the surface temperature of the PV module cooled by using different liquids was measured as 20 ^{o}C, and the temperature of the uncooled module was 29 ^{o}C. While the electrical efficiency of the PV module without cooling is

calculated as 11%, the electrical efficiency of the modules cooled using various fluids is calculated as 15% on average.

Key Word : Photovoltaic**,** Cooling, Thermal, Solar Air Collector, Electrical efficiency.

Science Code: 92802

ÖZET

Doktora Tezi

FARKLI TIP AKIŞKANLARLA YAPILAN FOTOVOLTAIK VE TERMAL SISTEM UYGULAMASI

Ismail ALBARKI

Karabük Üniversitesi
Lisansüstü Eğitim Enstitüsü
Enerji Sistemleri Mühendisliği Anabilim Dalı

Tez Danışmanı:
Prof. Dr. İlhan CEYLAN
Şubat 2021, 115 sayfa

Fotovoltaik modüllerin sıcaklığını düşürmek modülden elde edilen gücü ve modül verimliliğini artırır. Bu çalışmada PV modüllerin verimliliğini artırmak için yeni bir uygulama denenmiştir. PV modüllerde soğutucu akışkan olarak hava yada modül arkasına yerleştirilmiş borulardan geçen sıvı akışkanlar soğutucu olarak kullanılabilir. Modüllerde kullanılan soğutucu akışkanın tekrar sistemde kullanılabilirliği belkide en iyi tasarımlardan birini oluşturacaktır.

Bu çalışmada PV modüller modül arkasına yerleştirilmiş sipiral borular vasıtasıyla farklı akışkanlar kullanılarak soğutulmuştur. Soğutma sırasında ısınan sıvı akışkan ise tekrar aynı system içerisinde Kış mevsiminde ısınma amaçlı kullanılan havanın ısıtılmasında değerlendirilmiştir. Kış mevsiminde yapılan deneyler sonucunda farklı sıvılar kullanılarak soğutulan PV modülün yüzey sıcaklığı 20 ^{o}C iken soğutulmamış modül sıcaklığı 29 ^{o}C olarak ölçülmüştür. Soğutma uygulanmayan PV modülün elektriksel verimi %11 olarak hesaplanırken çeşitli akışkanlar kullanılarak soğutulan modüllerin elektriksel verimleri ortlama %15 olarak hesaplanmıştır.

Anahtar Kelimeler **:** Fotovoltaik, Soğutma, Termal, Güneş Enerjisi Toplayıcı, spiral boru PV / T, Elektrik verimliliği.

Bilim Kodu **:** 92802

ACKNOWLEDGMENT

My thanks and appreciation, and my great gratitude to his Excellency Prof.Dr. İlhan Ceylan, who supervised this thesis study, offered me all the help, direction, and mentorship all through the different phases of my examination work.

I wholeheartedly thank my family, especially my wife, for creating a good atmosphere throughout the writing of my letter.

With all love ... to my companion, my path, to the one who marched with me towards the dream ... systematically, we showed it to gather. We harvested it together and we will stay together

My sincere thanks to the supervising committee, Prof. Dr. Sezayi YILMAZ and Asst. Prof. Dr. Ali CAN, who provided all the advice and guidance until we got this work to the fullest. My thanks also go to Assoc. Prof. Dr. Alper Ergün, who followed me during lab work.

I do not forget; the Energy Lab staff at the University of Karabuk for their help in preparing for the experimental preparation and the probationary period.

CONTENTS

Page

Page

Page

Page

LIST OF FIGURES

Page

Page

Page

LIST OF TABLES

Page

SYMBOLS AND ABBREVIATIONS INDEX

LATIN SYMBOLS

PV : Photovoltaic

PV/T : Photovoltaic and thermal

FF : fill factor

A : area (m^2)

C_p : specific heat (J/ (kg K))

Et : rate of electrical energy (W)

I(t) : incident solar intensity (W/m^2)

$\dot{m}$: mass flow rate (kg/s)

$\dot{Q}_u$: rate of useful energy transfer (W)

T : temperature (◦ C)

P : power (W)

C : solar cell

a : availability

g : glass

i : inlet

m : module

o : outlet

Sc : solar collector

th : thermal

UV : Ultra-violet

V_{OC} : open-circuit voltage.

I_{sc} : short-circuit current.

PD : Theoretical power from solar system (Watts)

G : Constant Solar radiation (W/m2)

Y_{pv} : is the rated capacity (kw).

$f$pv : PV dating factor (%)

I_m : model current.

V_m : model volt

Psite : Measured Power from Solar.

T_{cell} : Panel temperature.

T_{amb} : Air temperature.

Greek letters

αp : Temperature coefficient of power (ºC)

λ : wavelength(m)

f : frequency

β : represents the temperature coefficient.

E_{xin} : exergy rate of inlet air (kJ/s)

E_{xout} : exergy rate of outlet air (kJ/s)

E_{xw} : exergy rate of wall heater (kJ/s)

E_{xd} : in total exergy rate into the dryer(kJ/s)

Ƞ : efficiency

P_f : Density of base fluid (kg/m^3)

Abbreviations

BOS : Balance of System.

MPPT : Maximum Power Point Tracker

NOCT : Normal operation cell temperature

STC : Standard Test Conditions.

BOS : Balance of System. PWM : Pulse Width Modulated.

HCPV : Heating Ventilation and Conditioning.

CHAPTER 1

INTRODUCTION

1.1. BACKGROUND

Energy is relating to development in many sectors such as agriculture, industry and transportation. It is one of the important factors in economic, social, environmental and human development. Energy and its accessibility are a prerequisite for social development. Therefore, the demand for energy increases dramatically every year. Much of this energy is obtain from conventional energy sources, especially coal and natural gas. The use of traditional fossil-based energy sources poses some problems. These energy sources are responsible for environmental problems such as air pollution and global warming impacts. It also leads to social problems such as health problems and a poor quality of life for communities. To prevent all these environmental and social problems caused by burning fossil energy sources, researchers have focused on renewable energy sources [1].

The interest in solar energy has increased dramatically, and scientists have developed new technologies to take advantage of renewable resources. Solar energy has used in many applications since its inception, the most important of which is heating applications.

Where solar radiation converted into liquid as thermal energy using solar collectors. Moreover, it was the most used liquid water, because it has a high heat capacity [2, 3]. Today, air has entered as an alternative in some applications. However, water is preferred because it transfers heat well. In addition, the increasing energy need was the efficient use of solar air collectors in different regions. The efficiency of these cells

varies from 10% to 20% in commercially used silicon cells.
This value reaches up to 40 % in sophisticated multi-junction cells [4]. In other words, almost 80 % to 90 % of the energy absorbed in a PV cell released to the environment as heat energy. With the increasing cell temperature, the photovoltaic module efficiency decreases significantly.

1°C increase in the operating temperature of the cells reduces efficiency by 0.5 %. To prevent this situation, cogeneration applications in which PV cells cooled and the heat is utilized in another process have become very popular.

According to Teo et al., the solar/thermal hybrid system applied. In order to minimize the temperature of the PV modules, the back of the PV module was fitted with an air duct arrangement in this experiment and an efficiency improvement of approximately 14 percent was achieved [6]. Previous research, Du et al., focuses on the use in CPV systems of active fluids cooling and the result shows that the power output increases as the unit temperature drops below 60°C [7]. To overcome the problem raised by the overheating of the PV module, several other efforts are underway. In Hosseini et al, an experiment was planned and implemented for greater efficiency.

The efficiency obtained was generally higher than the usual arrangement [8] where the energy extracted is directed in a limited order from the fluids used for cooling for another purpose in order to prevent waste. An effort to reduce the temperature of the PV module using the mounted Fluids pump has been carried out for several years in Cordzadeh.

The Fluids pump in this experiment serves as a cooling source for the fluids of the device. The results showed a great improvement in the PV module and overall performance. In addition, in Rosa-clot et al, the efficiency of the PV module implemented when immersed in White Spirit; a substantial increase in power output was achieved [10].

The chillers behind the solar panels were installed by Furushima and Nawata for the PV modules and allowed them to cool through the small holes in the cooling medium behind the panel flow. To steer the fluids towards the PV module, use this model. The cooling of the PV module improved the efficiency and power of the PV module and allowed hot Fluids to generated for testing [8].

1.2. PV/T LIQUID SOLAR COLLECTOR

The fundamental water-cooled configuration utilizes channels to coordinate liquid stream piping funneling joined straightforwardly or in a roundabout way to the rear of a PV module as shown in Figure1.1. In a standard liquid-based framework, a working liquid, ordinarily water, glycol or mineral oil flows in the warmth exchanger behind the PV cells [4].

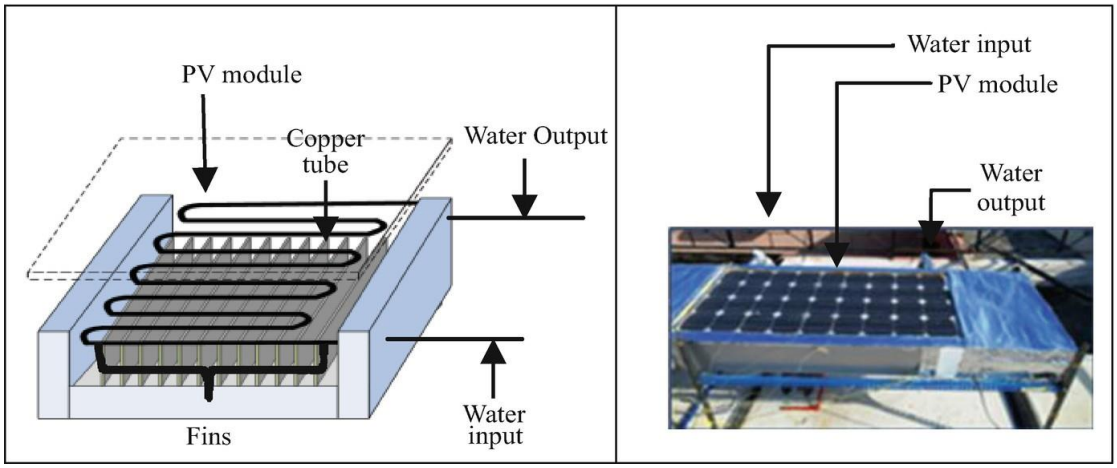

Figure 1.1. Schematic cross-sectional view of hybrid PV/T air collector; (1) simple configure ration; (2) studied configure ration.

1.2.1. Air Collector Photovoltaic Thermal

The layout fundamental for cooled much less air uses a hollow metallic casing conductive for the setup of PV panels, Figure 1.2. The warmness had launched of panels to the in closed area, thus the air both flowed to the air conditioning framework to recoup warmness electricity, nor it rises and blows from the top of the chassis [5].

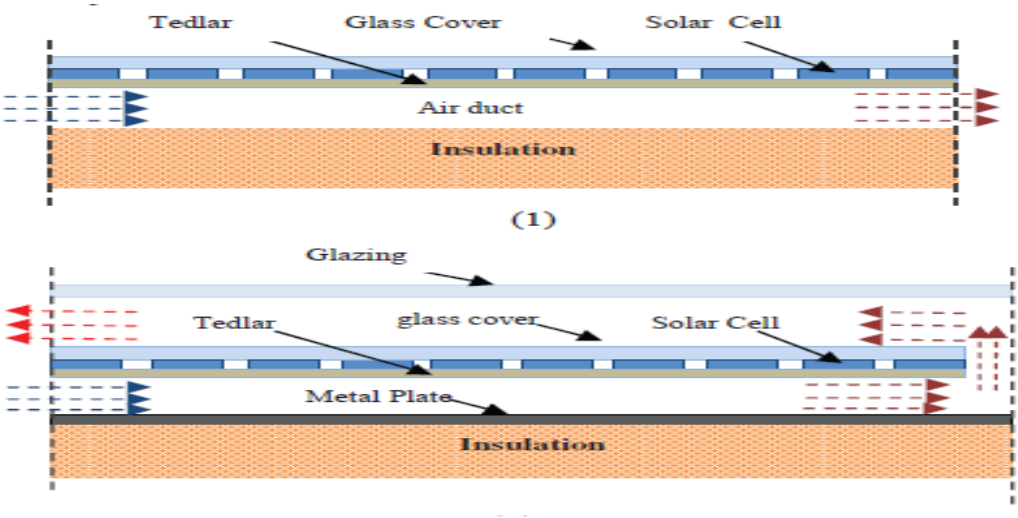

Figure 1.2. Schematic cross-sectional view of hybrid PV/T air collector; (1) simple configure ration; (2) studied configure ration.

1.2.2. Cooling Panel

The technique for introducing the boards assumes a significant job in guaranteeing great ventilation of the boards, which helps at reducing temperature of the panels, as it recommended installing the panels on the surfaces,150cm above the ground [6]. Water can also use directly because the outer face of the panels is of glass and after exposure for a long time to sunlight, the glass in turn will heat up and thus the use of water directly may lead to cracks in the glass that may be small at first but will cause greater damage over time. The choice of panels made of light panels also contributes to reducing heat absorption and thereby reducing the temperature rise of the panels [7, 8].

1.3. THE OBJECTIVE OF THE RESEARCH

Within this study the following objectives will be achieved:

- Decrease the effect of heat on solar panels.
- Extracting the best fluid in cooling the solar panels.
- Pave the way for research in the use of fluid and air in the cooling of solar panels

CHAPTER 2

LITERATURE REVIEW

2.1. INTRODUCTION

The fossil fuel for energy had depleted, polluted and rapidly consumed by the environment, researchers have sought new, unsustainable sources such as solar energy. Scientific studies have sought to perfect the efficiency of solar panels while decrease their economic cost [9], contributing to the prevalent utilize of panels solar. The productivity of solar panels contributes to finding scientific solutions that contribute to raising efficiency, which leads to the use of fewer panels with high productivity, which leads to lower economic cost. An important factor affecting the efficiency of solar panels is the temperature of solar cells [9], it known that with the hours of Solar radiation surfaces on solar panels, which leads to increase the temperature, which leads to reduced productivity, and therefore scientists turned to several ways to cool solar cells.

2.2. HIGH TEMPERATURE EFFECT

Several studies have carried out on solar panels, which have shown to lose their efficiency because of temperature changes and the degree of change between 1.7% and 11.3%. The highest temperature was 30°C at that time, this leads to a great loss in the efficiency of the solar panels, and therefore the cooling of the cells raises their efficiency by less than 3%. By placing tubes behind the cell for cooling, this reduces more than 10°C. This proposed arrangement can reduce its temperature by 20°C. These cells are electronic solar cells that convert sunlight into clean energy. That temperature has a huge influence on decrease the resulting capacity from cells as the data of cells written by manufacturers is not reliable, because they are at temperatures

of 25 degrees Celsius while the actual operating conditions in the summer months reach the highest grades.

Teoh et al (1983) they performed several experiments. As for none of cooling, the temperature and efficiency increased between 8% and 9% only. In the case of cooling, the temperature decreased significantly, which increased the efficiency between 12% and 14% Figure 2 1. [10].

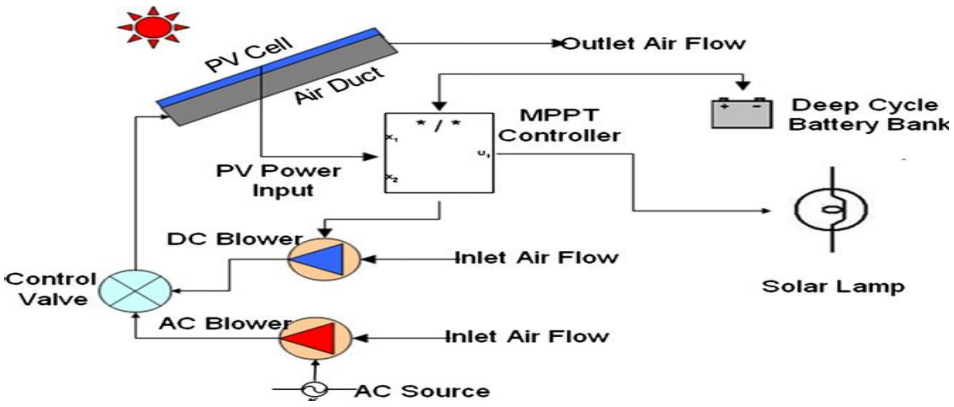

Figure 2.1. A schematic diagram of the experimental set-up.

Moharram et al. (2013) Researchers have designed a water-based cooling system for photovoltaic panels up to a maximum temperature of 35ºC. Based on this proposed system, it was found that photovoltaic panels produce the highest production capacity when the temperature reaches 45° C. Figure 2 2 [11].

Figure 2.2. Experimental setup 1. PV module, 2. tank, 3. pump, 4. filter, 5. nozzle and 6. drainpipe.

2.3. PV/T SYSTEM BASICS

Cells photovoltaic through which sunlight has converted directly into electricity, the materials of those cells are either a crystalline cloth inclusive of Crystalline Silicon or a non-crystalline fabric including Silicon an amorphous(a-Si), Cadmium (Cd), Indium Copper Dieseling or materials that are deposited as layers above Semiconductors are made up of gallium arsenide (GaAs). Figure 2.3 this image describes elements of the system from smaller to larger [12].

The intensity of the sun for a longer period has affects current generation just as its density. It also influences the effectiveness of the cell in changing over solar energy into electrical energy. When solar cells had connected in series, they give hundreds of volts of DC. The resulting energy can also be stored in lead or base acid batteries made of nickel and cadmium metals. Invertor reflectors for use and management of normal domestic and industrial electrical appliances can convert DC to AC. Of its advantage, that it does not have moving parts subject to disruption. Therefore, they work on satellites very efficiently, especially since they do not need maintenance, repairs or fuel. They work in silence, but Pollution and dust have reduced solar cell efficiency,

which requires us into ensure regular cleaning.

Exploiting the direct heat of the sun is another way to generate electricity from solar.

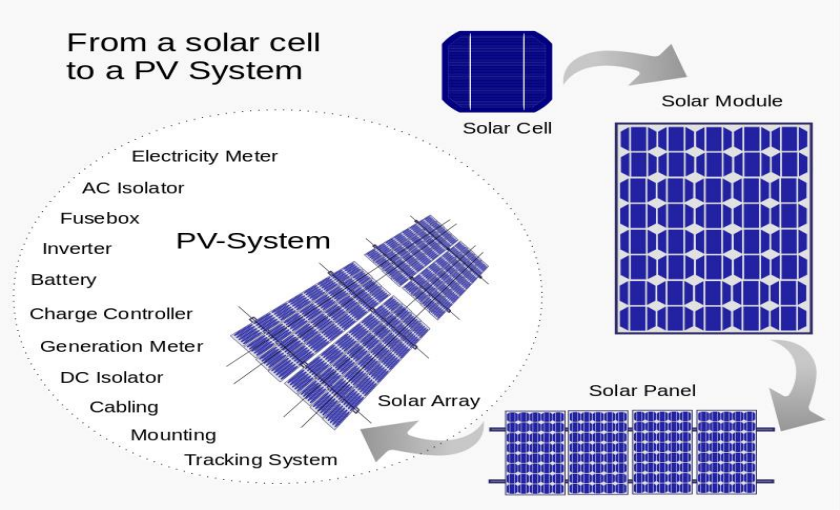

Figure 2.3. This image describes elements of the system from smaller to larger.

2.4. CONCENTRATION PHOTOVOLTAIC THERMAL TECHNOLOGY

Solar energy systems also used for desalination of water. Figure 2.4 shows the PV energy desalination system [13].

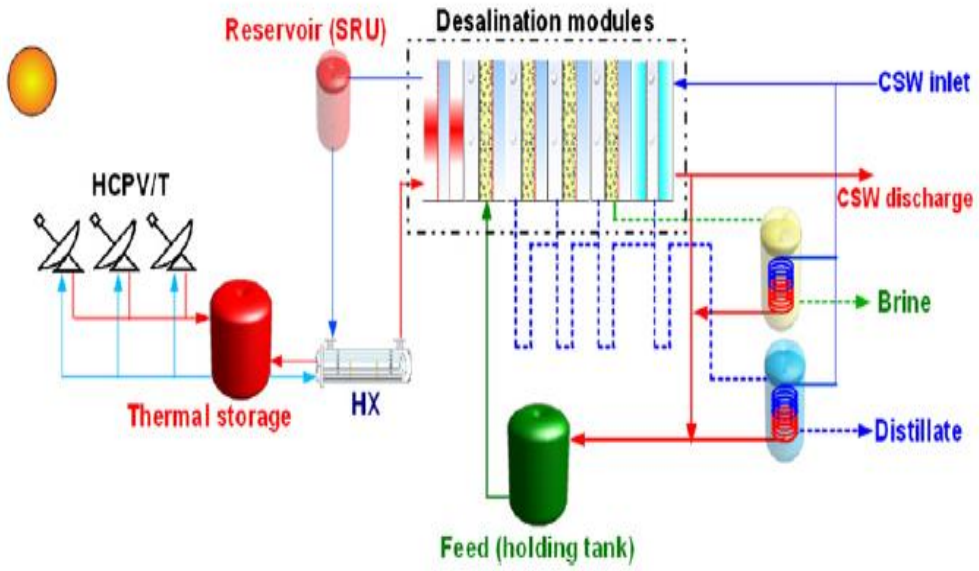

Figure 2.4. Process flow of HCPVT — desalination system (pumps and valves are not shown here).

2.4.1. Concentrator PV/T Technology

The advantage of the Concentrator system is minimizing number photovoltaic cells necessary. It as well decreases the concentration of solar radiation, which reduces heat loss to the surrounding environment, which greatly improves efficiency at high application temperatures [13].

Teoh et al (1983) Experiments had done with and without cooling Figure 2.5. Solar cells can only realize an efficiency of 8–9% without cooling. When temperature dropped under cooling condition; this leading to an increase in efficiency of solar cells to between 12% -14%. [18].

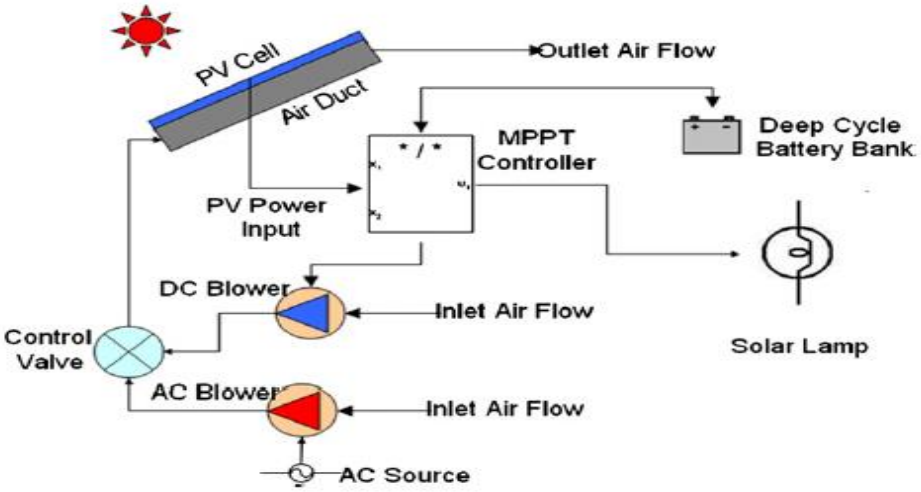

Figure 2.5. A schematic diagram of the experimental set-up.

Salim and Nunilo (1990) Researchers designed a large system, a large photoelectric compound (PV). They operated the system in several different modes and co-generated with diesel generators. The system will have an additional capacity to be directly coupled with electricity of 350 kilowatts to produce hydrogen [12].

Bhavnagar and Joshi (1990) the researchers performed the performance of the silicon cell-based concentrators at 40× for 3 years. It has collected unit power output. Temperature and Solar radiation have found that these concentrators are not suitable for Indian conditions because the panels are subject to degradation at 2-3% of the middle primary efficiency of 7% due mainly to the decrease. [14].

Royne et al (2005) the researchers Design systems cooling contain minimum and uniform temperatures cell, and lower power exhaustion by the system. According to geometry examined solar concentrators systems grouped. Cooling solutions for Single cells only need passive cooling, also for high solar concentrations. An active cooling system is necessary for densely packed cells under high concentrations (4150 suns). [15].

Kribus et al (2006) the researchers designed the system (MCPV); which has repetition in the output of electro and thermal Figure 2.6. This system is good because of studies and considered something new in terms of heat transfer system, electrical and thermal performance, manufacturing cost, and the resulting results. When analyzed cost energy in water heating domestic [16].

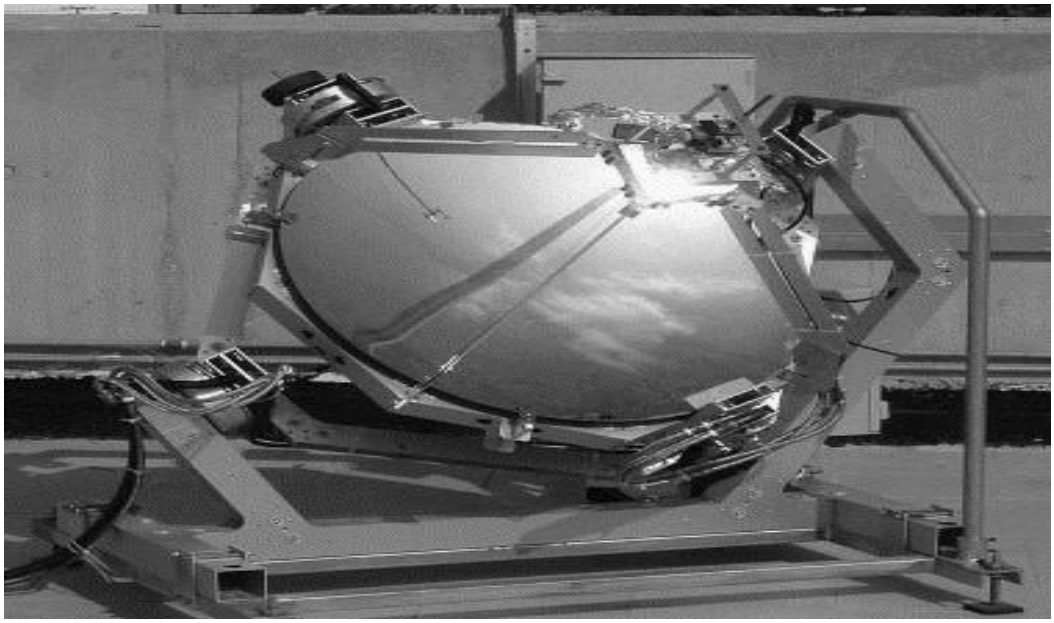

Figure 2.6. The MCPV unit during solar testing.

Sangani and Solanki (2007) the researchers designed and built V-trough concentrator photovoltaic systems. Figure 2.7 to reach a decrease in the cost of electricity. Then develop a capacitor system for various sort of tracking process. The V-trough capacitor system with an engineering concentration output power increases by 44% compared to the passively cryogenic surface panel PV. Low-angle design models gave higher power produce due by high permeability of the glass [17].

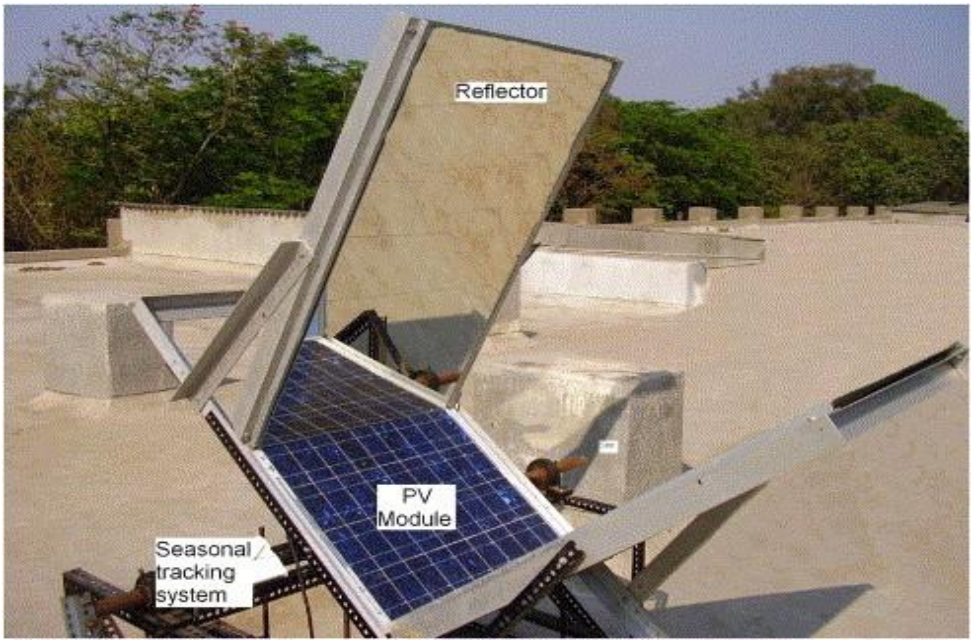

Figure 2.7. V-trough concentrator system.

Aladdin Mokri, et al (2011) Researchers have shown the actual situation of PV technologies and the intensive marketing. They determined capacitance of CPV in the world based on the latest industrial reports in 2010, which was about 21 MW. The lower installation price around $ 3.05 / watt and flat price electricity lower $ 0.14 / kWh. The conclusion drawn from the study is that high-focus CPV systems have higher economical possibility compared to lower concentrate systems CPV. [20].

Radermacher et al (2012) Researchers use the hybrid assembler to drive a hybrid air conditioner that separates underlying and reasonable loads. The heat output from collector are power through the electrical output powers. System achievement prepared using the systems emulation plan in Abu Dhabi.

The results showed that the separation of Latent cooling load and sensible loads had active in wet, and temperature demands of buildings in hot and wet climate. Additionally, the performance of the suggested system is higher during the year unless in another. [21].

Rizwan Arshad et al (2014) in this paper, the researchers explained that mirrors and the cooling process had improved solar panels efficiency. The experimental results indicated a noticeable enhancement in output of the solar panels as:

- Without cooling and reflectors.
- Without cooling with reflectors.
- a comparison of between reverses and cooling.

Results showed in case B 32% efficiency improvement to 52%. while case of C it is scheduled and drawn [22].

Mr. Santiago (2015) the researcher worked on CPV technology, and he reduced manufacturing Costs. This will positively affect the initial investment costs. The low cost of self-sustainment and self-sufficiency, and reduced space requirements for same energy stabilization, give CPV and HCPV technology an edge over other renewable technology. [23].

A. Muthu Manokara et al (2016) in this paper, researchers worked on combining two systems: a basin equivalent as capacitor and a receiver the PV / T channel. Figure 2.8. As well as studying the achievement of concentration the parabolic trough, PVT is made and rated by flow water with concentration PVT. [24].

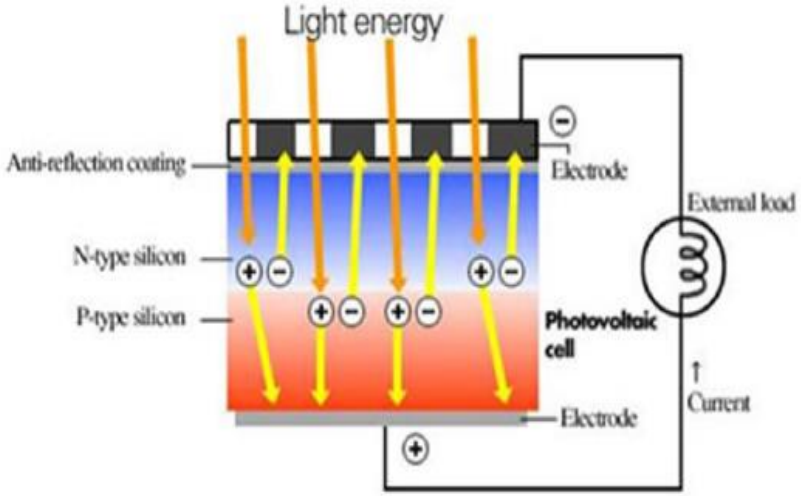

Figure 2.8. Photovoltaic cell generates electricity when irradiated by sunlight.

2.4.2. Air Type PV/T Systems

Researchers in these fields carried out several research and experiments that had a role in development. They are as follows:

Sopian et al (1996) the researchers measured the achievement of the single and high pass aggregate photovoltaic assemblies and the fluid used was air. The models had established at energy saved at the different points the collector. Comparisons had made through the
achievement of two kinds from photovoltaic complexes. The outcome showed a new designing of the dual thermal collector with best achievement. [26].

De Vries (1998) The researchers designed four simulation digital models for the photoelectric heat sink assembly with a three-dimensional unique model and three static case models: D1, D2 and 3D. The outcome was compared to the experiential results. all models had followed up tests with 5% fineness [28].

Khaled Touafek et all (2013) Researchers have studied to design a new PV/T hybrid

complex. The absorbent used is made of galvanized iron and is inexpensive (compared to copper) and for the novel complex mathematical model has been advanced. beneficial thermal power was about 290 watts while heat efficiency was about48%. [36]

Cătălin George Popovicia et al (2016) the researchers presented a digital methodological study to reduce the photovoltaic temperature using air-cooled thermal depot. The geometric shape of the model, Figure 2.9, was accomplishes using the ANSYS - Design Modeler. The model utilized to simulate solar is Eluent's solar beam tracing niche. The calculation Reynolds is around 13100, for a prescribed speed of 1.5 m/s [37].

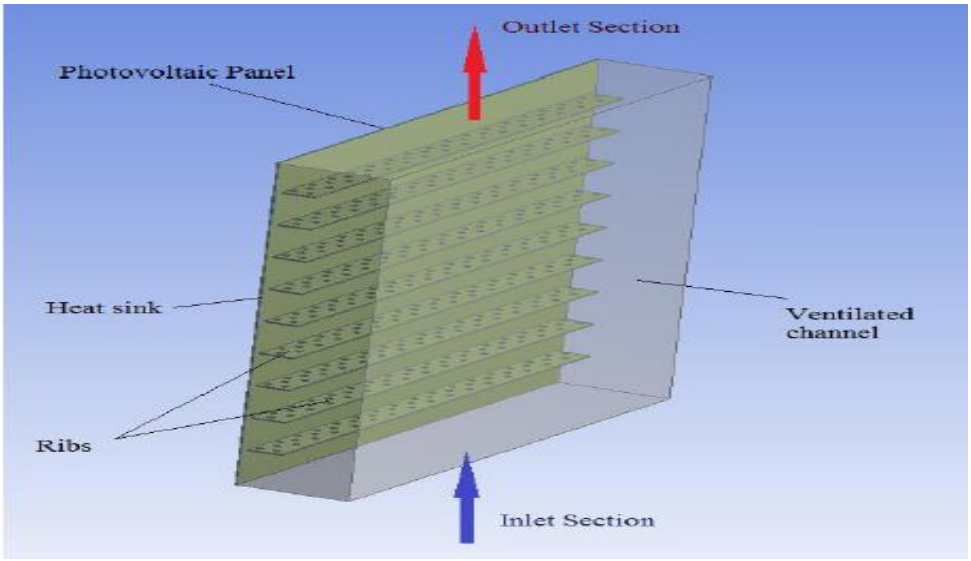

Figure 2.9. Geometry of the studied model.

2.4.3. Type PV/T System

Soteris A. Kalogirou (2001) Researchers designed a simulation sample with PV/T Figure 2.10, the model shown to consist of a set PV panels and a battery and reflector. Researchers reached the following results, which is the optimal water flow average for system is 25 L/h. Hybrid system raise average yearly efficiency of solar from 2.8% to

7.7% Addition to covering 49% from hot water for the house, thereby raising the average yearly system efficiency to 31.7% [39].

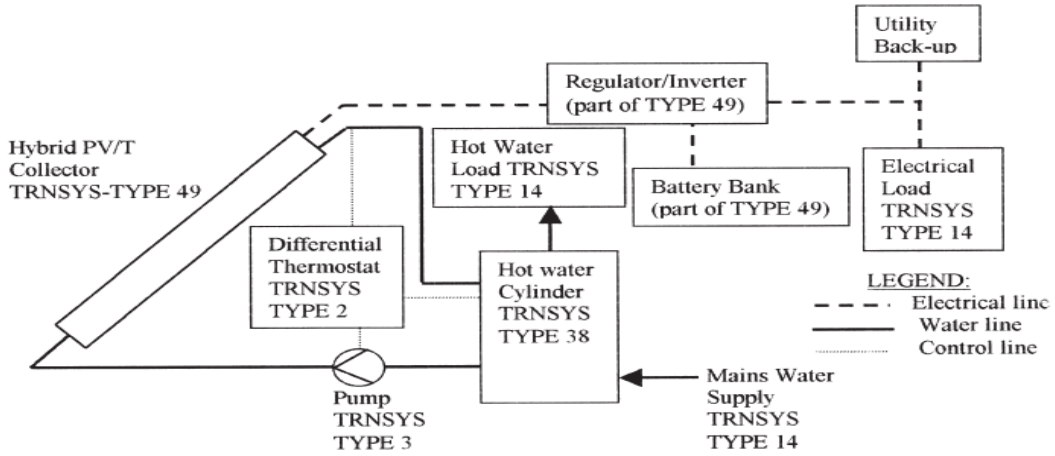

Figure 2.10. Hybrid PV/T system schematic.

Zondag et al (2003) this study about a clear view for different concepts of the combined photovoltaic complexes. The researchers evaluated nine concepts that ability categorized into four groups.

Where a case of all group is set at Figure 2.11

- PVT Plate and pipe collectors.
- PVT Collectors canal.
- collectors free flow.
- PVT with two absorbers.

The photoelectric design below gives the best efficiency channel, it showed that into the naught temperature, the thermal efficiency from the open complex is 52% and the thermal efficiency for the design of odd-overlay panels and tubes is 58%, whereas the canal over the photoelectric styling usually has 65% thermal efficiency [41].

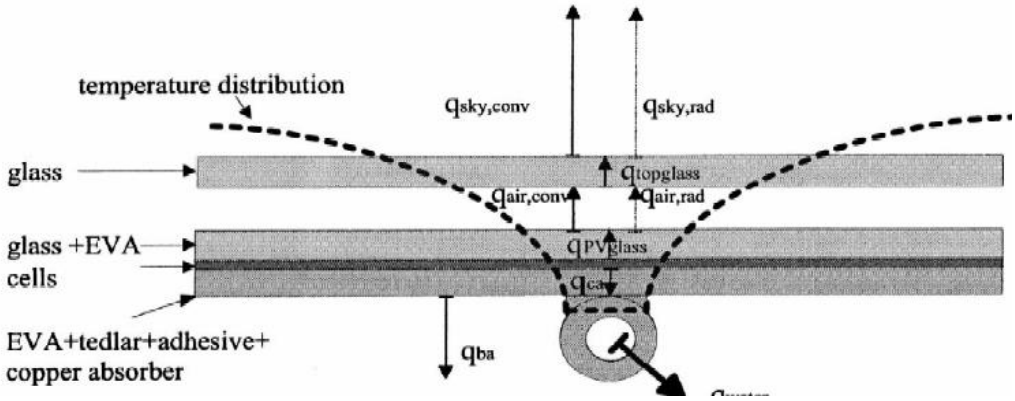

Figure 2.11. Cross section of kombi-panel. The material layers in the kombi-panel are indicate, as well temperature and the various heat fluxes.

Li Zhu (2010) in this study the system consisting of a liquid submerged CPV plate consists fundamentally of a two-axis track capacitor. Figure 2.12, a liquid-obscure receiver and other auxiliary accessories. Experiential outcome shows that the temperature of the module maximum to. 49°C and the symmetry of the temperature division is less than. 4°C at 250 sun with a DNI greater than 900 W/m^2, the average inlet temperature is around 31°C and the temperature is The room is about 17ºC. [48].

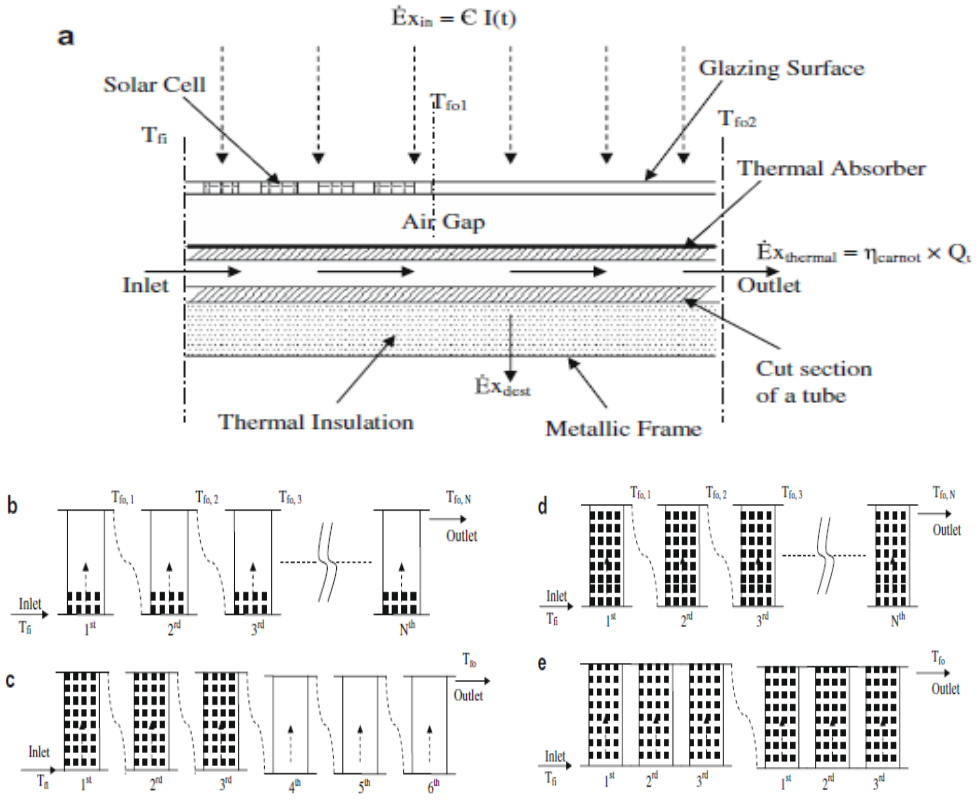

Figure 2.12. Cross sectional collector partially (b) Collectors partially. (c) Collectors fully (d) Collectors fully (e) Series and parallel combination of collectors.

Amit Sahay (2015) this study conducted by the researchers discussed various technologies of solar PV panels cooling and the testing. This study showed that there is a noticeable raise at the transference efficiency due to the cooling of the PV panels. ANOVA is used in data analysis to determine the causal effect of refrigeration action Figure 2.13 a. b.c.d [51].

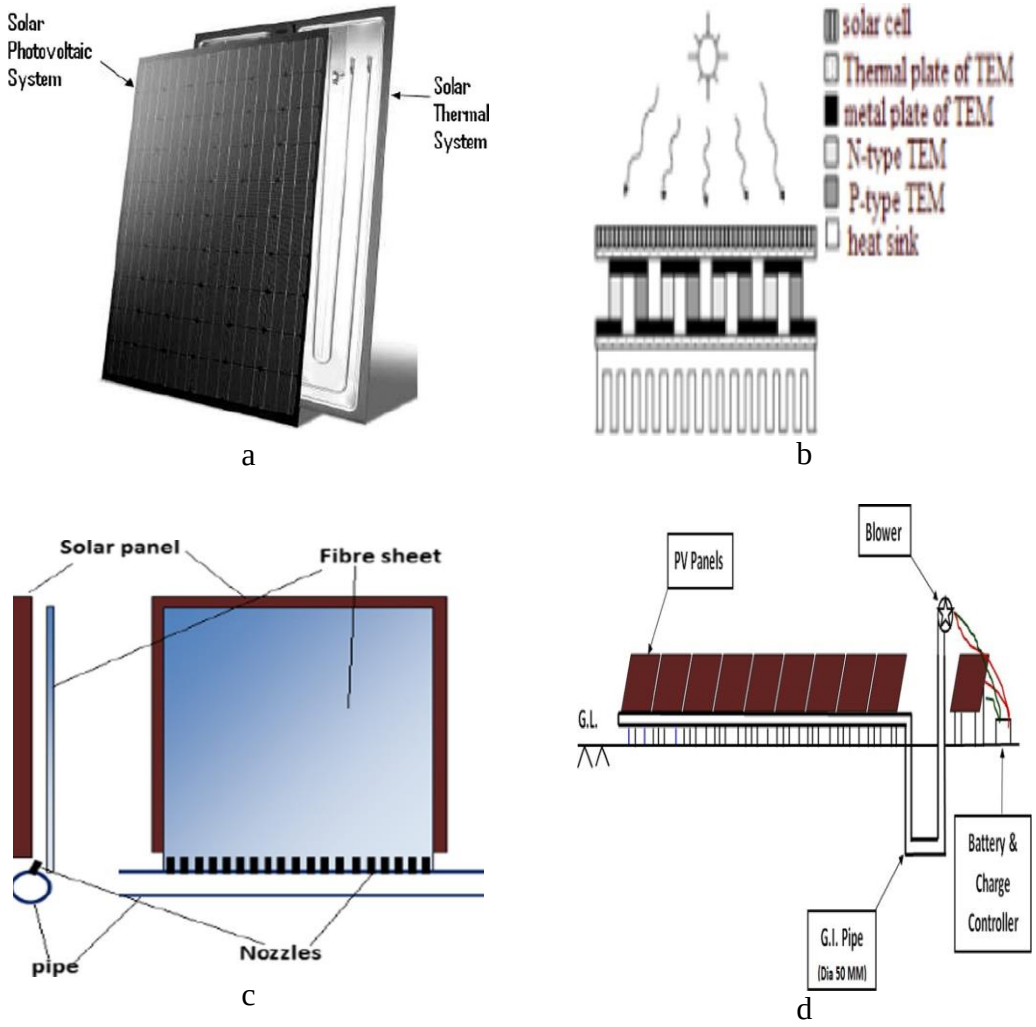

Figure 2.13. Schematic design.

J. Siecker et al (2017) The researchers studied various methods that they utilized to reduce the passive effects of the raised temperature to progress the efficiency of solar panels in the case of temperature, except for the standard test (STC). The results of this study are to save the operating room temperature least to improve the overall energy efficiency [53].

Nasser Ahmad et al (2018) the researchers introduced a new design for a water-based photoelectric cooling system to lessen the effect of high heat. Figure 2.1**4**. After performing the experiments, the results showed the water gathered from the plate next

40 minutes of cooling obtained a heat of approximately 10°C, which improved the efficiency by 10.35% (do not the use of MPPT) utilized water at an ambient temperature (24°C) compared to the non-plate Refrigerated. In addition, during the peak solar hours, the plate temperature decreased from 64.3°C to 32°C and from 59°C to 27°C in 3 minutes with the back and front roof, respectively.

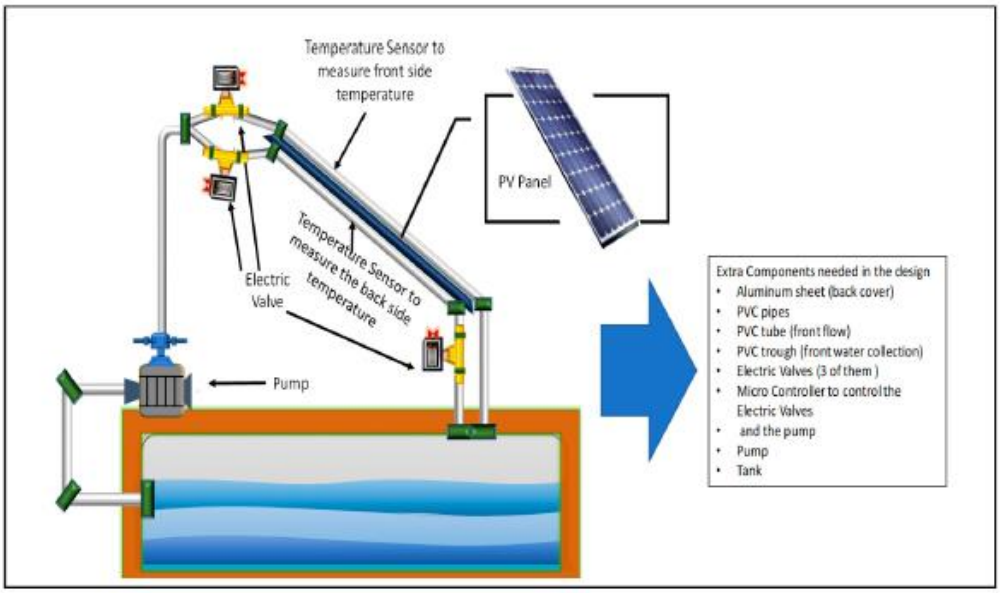

Figure 2.14. The configuration of the experimental setup.

This study had designed and construct a PVT experimental model and we used in this model three fluids (water - aspirin - alcohol) with respect to PF, for the solar collector, air was used.

Use a heat exchanger for the model. The system performed well around 7%.

CHAPTER 3

PHOTOVOLTAICS PV AND PV/T TECHNOLOGY

3.1. SOLAR POWER DEVICES

Solar Photovoltaic power can have identified as the electricity generated from the solar photovoltaic cell. Solar cell converting the sun light directly to electricity allow into the photovoltaic effect, wherever picture means the light and voltaic means electro. The solar cell is made of a cured silicon semiconductor, known as a silicon photovoltaic solar cell. first generation solar cells type of technology is also known as classified into monocrystalline and polycrystalline, now a day are still the most favorable types used in the global market [3].

Solar power become now same as wind power, the most viable and environment friendly source.

3.1.1. Properties of Light

The solar sun energy has many forms of radiation apparent light, UV ray or infrared ray IR ray, as we can see from figure 3-1, around half of Sun power in the Visible light zone. Visible light sees as (a few subsets of the electromagnetic spectrum ago the late 1860s) [56].

The light characterizes by electromagnetic spectrum as [uninterrupted number of

waves with various wavelengths], as shown in Figure 3.1. The Relation between wavelength λ (m), and frequency *f* (Hz) could express as following formula:

$$f = \frac{C}{\lambda} \tag{3.1}$$

Speed of light: C = 3 × 10^8 m/sec.

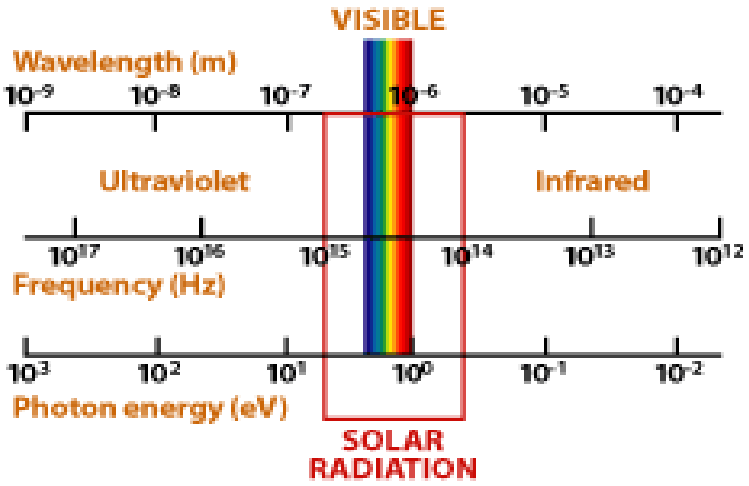

Figure 3.1. around half of Sun energy in the Visible light region.

3.1.2. Spectrum Solar

The wavelengths of sun emit most of its energy in a range from 2×10^{-7} to 2×10^{-6} meters. It is being described as the shortened the wavelength is the higher the frequency and the greater the energy (expressed in eV).

The Relation between photon energy *E* and the wavelength can have written as follows, figure 3.2.

$$E = \frac{hc}{\lambda} \tag{3.2}$$

Planck's constant h (= 6.626×10^{-34} Joule· sec) [56]

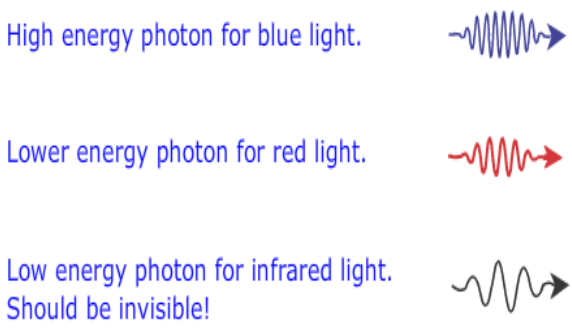

Figure 3.2. High energy for Blue light photon.

3.1.3. Standard Sunlight

Sunlight Standard condition at a net day at the equator at noon called full sun, which is, gives an radiation of 1000W/m^2, at this amount of radiation intensity the current of typical PV cell will be at the maximum, as we can see from figure 3.3.

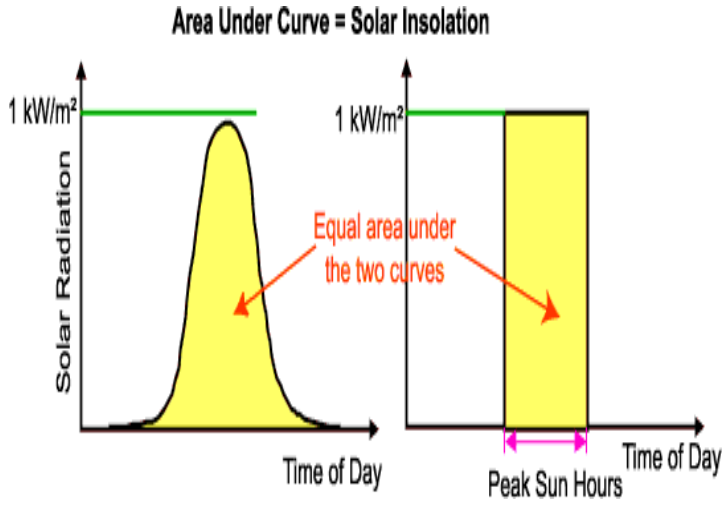

Figure 3.3. Standard sunlight conditions (1000 W/m2) "full sun."

If the radiation is 500W/m^2, the amount from product current roughly cut off in half, also named as one-half of the sun energy.

Full sun term refers generally as various photovoltaic solar cells manufacturers to “maximum output power”, “peak power” and “maximum power point” [57].

3.1.4. Solar Cell

PV Devices that convert light into electricity direct (DC). We can be connecting set of PV cells into modules. Typical 12V module consist of 36 cells 18 V, 2.7 A.
The modules and arrays used to charge battery bank or potential any digit of electric loads on an off-grid system via solar charge controller and off grid inverter. Also, these modules and arrays can interconnect to the utility grid, called on grid system by using on grid inverter, this system ranged from few watts to megawatts. The inverter output alternating current (AC) compatible for each classic appliance [58].

3.2. A TYPICAL SILICONE PV

A model silicon PV cell is composed of a tender wafer consisting of an ultra-thin layer Silicon phosphorous (type N) on top of a thicker layer of silicon (type P). Where an electric field is close to the upper surface of the cell so that the two materials are in contact. When sunlight falls on the surface of the cell, this causes current to flow when the solar cell is connected to an electrical load [59].

Ignoring the size, the silicon cell produces about 0.5 - 0.6V DC under open circuit, and no-load conditions are seeing on Figure 3.4.

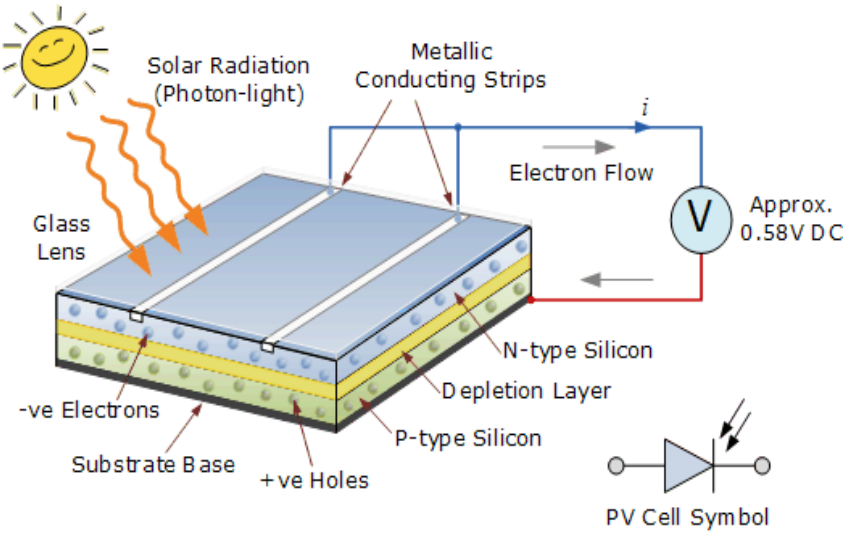

Figure 3.4. Diagram of a photovoltaic cell.

The efficiency of a photovoltaic cell depends on its output and also the surface area A, and the performance ratio PR and the intensity of sunlight striking the surface of the G cell (W/m^2) is as follows:

$$P_{pv} = G_{rad} \times A_{area} \times E_{effi} \, PR_{perf} \qquad (3.3)$$

3.2.1. Equivalent Circuit of Photovoltaic Cell

Photovoltaics known to be devices made of nearly silicon semiconductors such as electronic diodes and transistors [57]. The equivalent circuit of a typical cell consists of a current source in parallel with a diode (Figure 3.5a).

There are resistors to the real effects of a photoelectric cell represented in circuits, for example Figure (3.5b) includes the series resistor, and Figure (3.5c) includes the parallel and series resistances. Other embodiments include two binaries as in Figure (3.2d).

The equivalent circuit as Figure (3.5c) is commonly used, usually in simulations,

simplifies the high-value parallel resistance process Rp, as shown in Figure (3.5 d), as with many research, this circuit contains a model to simulate a solar PV cell.

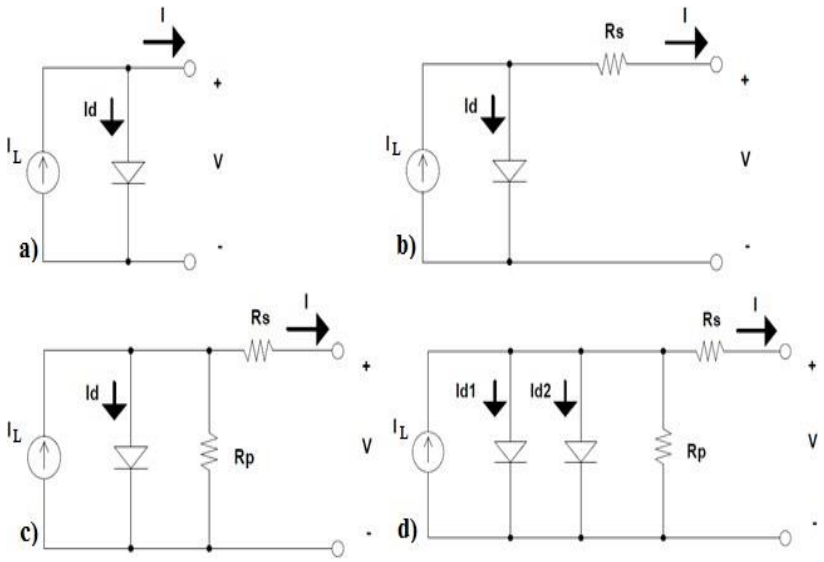

Figure 3.5. The equivalent circuits of an ideal cell.

According to the equation of an ideal cell, this can have expressed as follows:

$$I_L = I_D - I_L = I_S - I\left(e^{Qv/KT} - 1\right) \qquad (3.4)$$

IS stands for diode saturation current, q is 1.6 x 10-19 coulomb, k is Boltzmann's constant, 1.38 x 10 -23 J / K, T is the cell temperature in degrees Kelvin, and V is the cell voltage measurement [60].

3.2.2. Photovoltaic I-V Curves for Solar Cell

Voltage curves are most important issue to good understanding the real performance of cell or the module on site, the manufacturer often produce I-V curves to photovoltaic cell delivers current and voltage at maximum power output under standard conditions for the STC test, at 1000 W / m^2, 25°C and AM = 1.

At any point along the curve the solar PV cell power (Power = VI) as seen in Figure 3.6, the amount of radiation is the keystone to maximize output power from a cell, for this the experts' advice that the face of the photovoltaic should pointed as straight toward the sun as possible [59].

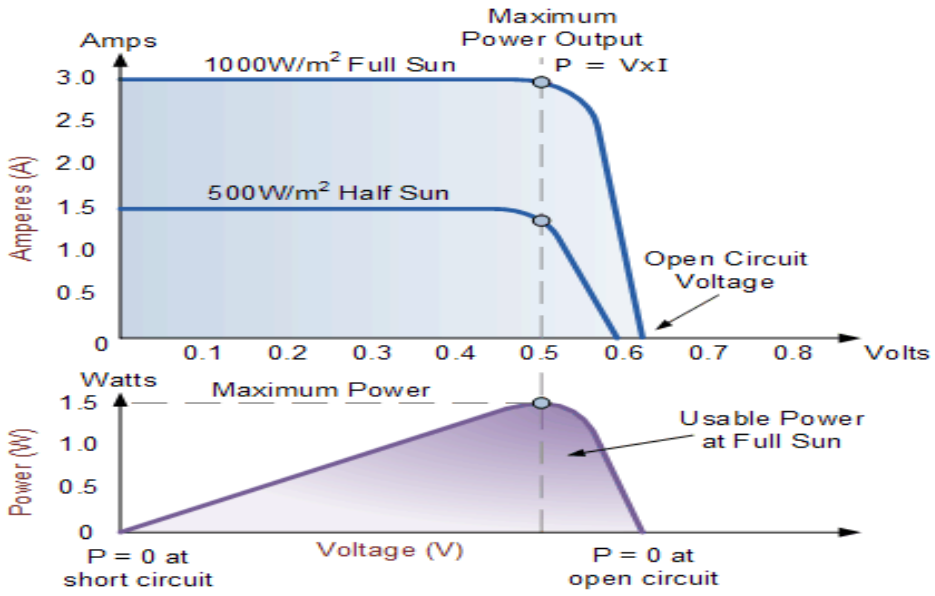

Figure 3.6. Photovoltaic Solar Cell, I-V curves, watts = volts x amps.

3.2.3. Solar Cell Voltage

The photovoltaic cell produces an open circuit (VOC) voltage of about (0.5 to 0.6 V) at 25 °C. As the solar radiation increases, the cell voltage remains constant, as shown in Fig.3.7.

When the cell is connected to a light bulb, for example as a load, the output voltage drops to about 0.46 volts, and then the electric current flows, Ignoring the radiation intensity, the voltage level remains constant. Resistance and energy loss within cells cause a decrease in output. [61].

The temperature of the cell is the second factor, as the higher its temperature the energy will decrease, it depends heavily on the material and the quality of the cell, but in

general, the output voltage decreases at midday as full sun, by 3% for every 25°C increase in cell temperature.

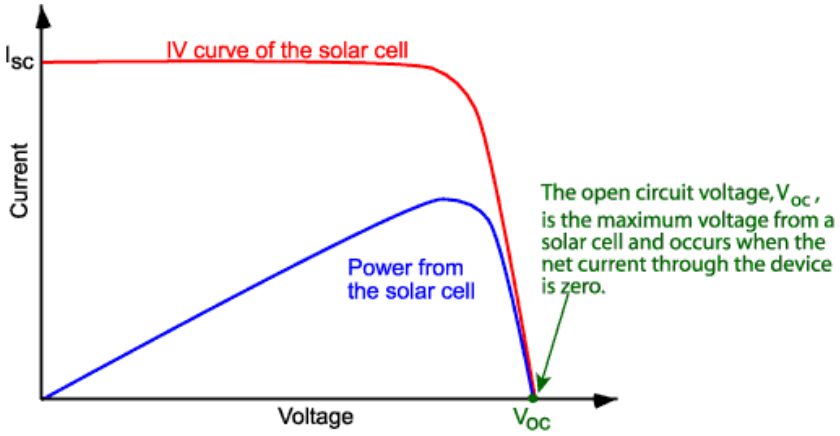

Figure 3.7. Open Circuit Voltage (VOC) for Photovoltaic cell.

3.2.4. Solar Cell Current

The photovoltaic cell, output DC curve as field measurements and previous studies has strong relationship to day sunlight or the amount of radiation fall on cell surface. If the sunlight is 1000W/m^{2}at standard condition, for 3A PV cell as example, the current will be in the maximum value, 3A, also if the radiation is low as 500W/m^2 the current will be 1.5A. This is because the amount of radiation is depending strongly to photon energy and type, the blue photon wavelength is shorter than red photon so blue color refers to day light with strong energy and red photon refer to sunset with no energy.

In addition, the larger the cell, the lighter energy entering the cell, because the output current is directly proportional to the surface area of the cells. Then the higher the cell production, the more sunlight entered the cell, [61].

In practice, we are carefully choosing the loads, which will have connected to solar cells because the cell current decreases rapidly as the load resistance increases figure 3.8.

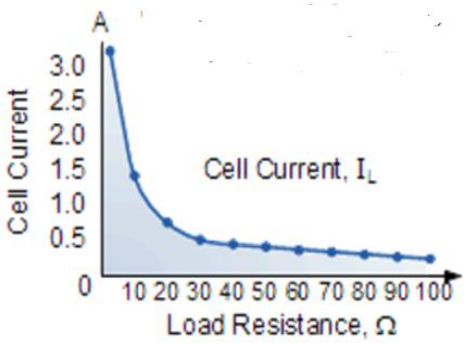

Figure 3.8. Cell current – Load resistance curve.

3.2.5. PV Panel Power Output

To determine the energy quantity of a solar cell in watts at site, we will use melty voltmeter devices (Voltmeter and current meter) to measuring the sell or module voltage and current, (Im and $V_{m)}$ the output power then will be equal for production measured the current voltage. As measurements the optimum operational voltage of PV cell under normal operation condition is close to (0.46) volts, generation a current of about (2.77- 3A) at full sun. The typical power output of a solar photovoltaic cell is estimate as follows:

$$P = V \times I = 0.46 \times 3 = 1.38\, watt \qquad (3.5)$$

If we connected 36 cells to achieve standard 18V, the module power will be 50W, if we are increasing cell number also voltage and current power increased. To PV module in factory. The group of cells connected to serial to get desired voltage of module (36 cells for 12-volt module and 72 cell for 24-volt module) and to achieve the required current, we conduct parallel connections to increase the current and voltage to add more power. On the practical side, this aspect shows the linear relationship between (I-V) linear relationships in the photoelectric cell. In short, circuits they provide approximately the same current.

3.2.5.1. Photovoltaic Cell Example No 1

If we connect ten PV cells, (0.46 V, 3A each), together in series to output photovoltaic module, output voltage will be (4.6) volts, but the current still (3A).

3.2.5.2. Photovoltaic Cell Example No 2

Commercial trade PV cell with a surface area of 160 cm2 (16×10 cm) will output about two watts' peak power under full sun (1000W/m^2). If the radiation were 50% of peak.

3.2.5.3. Photovoltaic Cell Example No 3

Determined the top output current of solar PV silicon cell with (0.5V), rated power (1.75W), at (1000W/m^2) full sun [62].

$$P_{\max} = V_{out} \times I_{\max} \tag{3.6}$$

$$I_{\max} = \frac{1.75}{0.5} = 3.5A$$

3.2.5.4. Photovoltaic Cell Example No 4

In the case of bright of sunlight, the photovoltaic cell produces (0.58 volts) and current (1.73 amps). We calculate the peak power output of the PV cell in watts.

$$P_{out} = V_{out} \times I_{out} \tag{3.7}$$

$$P = V \times I = 0.58 \times 1.73 = 1\ Watts$$

3.3. TYPES OF SOLAR CELL

Solar cells classified into several generations, which are the first, second and third generations, some sources include fourth generation, but other resources considering it as follower to third generation. The global solar PV installation now based on mono and poly crystalline modules up to 500 W, with little contraption for thin film type.

The first-generation cells are made of crystalline silicon, which also called conventional cells, which is the commercial technology for photovoltaics, which includes materials such as polysilicon and monocrystalline silicon.

The second-generation cells are thin film solar cells, which include amorphous silicon cells, CdTe cells and CIGS cells.

Likewise, the third generation of solar cells includes a number of thin-film technologies, often described as emerging photovoltaics, all of which are still in the research or development stage. As shown in table 3.1. Many use organic materials, which are mostly mineral oregano compounds as well as inorganic materials.

Table 3.1. Silicon cell types [63].

Type of Silicon Cell	The efficiency	Advantages	Disadvantages
Monocrystalline	15%-24%	durable, proven, aesthetically pleasing	Highest cost
Polycrystalline	12%-16%	Lower cost, improving efficiencies	Lower efficiency, poorer aesthetics
Thin film	7%-13%	Low cost, easy to make, best aesthetics	Low efficiency, less proven

3.3.1. Crystalline Silicon

Crystalline silicon (c-Si) is the most common bulk material for solar cells, and it called "solar grade silicon". Depending on the size of the crystal in the resulting ingot or

wafer, loose silicon separated into multiple classes. Cells based on the concept of a p-n junction. CCS solar cells are made of chips with thicknesses ranging from 160 to 240 mm.

3.3.1.1. Monocrystalline Silicon

(Mono-Si) is the most expensive cell of all cell types. In terms of design, the corners of the cells cut, because the wafer material cut from cylindrical alloys, which usually grown by the Chukralsky process. Solar panels using mono Si cells display a distinct pattern of tiny white diamonds.

During June 2015, the n-type monocrystalline silicon solar cells developed to an efficiency of 22.5% over a total cell area of 243.4 cm^2.

3.3.1.2. Polycrystalline Silicon

Polycrystalline silicon cells are large blocks of molten silicon finely chilled and frozen, which are made of square alloys. Polysilicon cells are the most widely used type of photovoltaic cells, their cost is low, and their efficiency is lower than those made of nanocrystals are.

3.3.1.3. Silicon Ribbon

The silicone strip is a thin, flat film of molten silicone, resulting in a polycrystalline structure. It also considers these cells cheap to make from the same poly crystals.

3.3.1.4. Mono-Like-Multi Silicon (MLM)

The model had founded at the year 2000 in the laboratory, and then could introduced commercially around 2009s, known as Cast-Mono, which is a design that relies on

polycrystalline molding chambers for few 'seeds' of one material. The result is a semi-monopoly material that is polycrystalline around the outer sides. This product results by monocrystalline- such cells at polycarbonate-as prices, thus minimizing the total cost with higher efficiency.

3.3.2. Thin Film

Most of the thin film designs have the lowest efficiency and temperature effect of first-generation silicon PV solar technology; it a technique that decreases the amount of effective substance in the cell. Most active ingredient designs sandwich inters two sheets of glass, for this reason it is heavy in Wight as twice as crystalline silicon modules. Most of universities researchers still developing it on the laboratory tests.

3.3.2.1. Cadmium telluride

Cadmium telluride is the only thinner material that competes with crystalline silicon in terms of cost / watt. Therefore, cadmium is very dangerous because it is toxic due to limited supplies. A square meter of CdTe contains approximately the same amount of cadmium as a single-cell nickel-cadmium battery.

It has the high efficiency (~ 20%). New developments in IBM and Nano solar are trying to reduce costs by using non-vacuum solution processes.

3.3.2.3. Silicon Thin Film

The most common thin-film technology is amorphous silicon. The solar cell has a band gap (1.1V - 1.7V) of crystalline silicon, which is optimal for high open circuit voltage. This cell absorbs the visible part of the solar spectrum more strongly than the high-intensity infrared part of the spectrum.

3.3.2.4. Gallium Arsenide Thin Film

GaAs cells are expensive; with 28.8%. [4] GaAs most generally utilized in multifunctional photovoltaics for centered photovoltaics (CPV, HCPV) while solar modules over spacecraft because the industry prioritizes efficiency over the cost of space solar energy.

3.3.2.5. Multifunction Cells

Multiple junction cells made up of several thin films, every being a developed solar cell, generally using organometallic vapor phase epitaxy. The three-junctional mutant cells reached a record high of 44% on October 15, 2012.

In 2016, a modern process for the production of hybrid photovoltaic panels was described, which combines the rise efficiency from III-V multiple solar cells for economy.

The number of person photovoltaic cells required perfect a single photovoltaic solar module consist on the amount of electricity required.

Figure 3.9. Photovoltaic modules.

Most standard solar panels have an output voltage of 12 volts and 24 volts. Standard 36-cell silicon crystalline solar panels had designed to charge a 12-volt battery.

A model 12-volt photovoltaic provides approximately 20.8 volts' power utilize 32 or 36 separate cells united in one embodiment.

Solar panels have an output of 24 volts, so there are 64 or 72 separate cells in one panel. It has an open circuit voltage (VOC) which is much higher than the mid-30s and has a higher peak power of between 150W and more. [63]

3.4. PV- MODULES LAYER

All PV modules consist of several coat with the light side facing back in Figure 3.10:

- **Layer Protection:** It is usually glass, but in thin films, it is transparent plastic.
- **Contact Front:** The electrical contact in forehead must be clear.
- **Material Absorption:** Absorbing material: The materials used are

semiconductors and have a layer in which the light is absorbed and transform into an electric current. Moreover, there are various layers of different substances to improve performance.

- **Contact mineral back:** A jointer support completes the electrical circuit.
- **Film Laminate:** A laminate includes while structure is waterproof and isolate from heat.
- **Glass Back:** This coat provides safeguard in the back from the module. Can be glass, aluminum or plastic.
- **Connectors:** Finally, unite had equipped with connectors and wire so it can have wired.

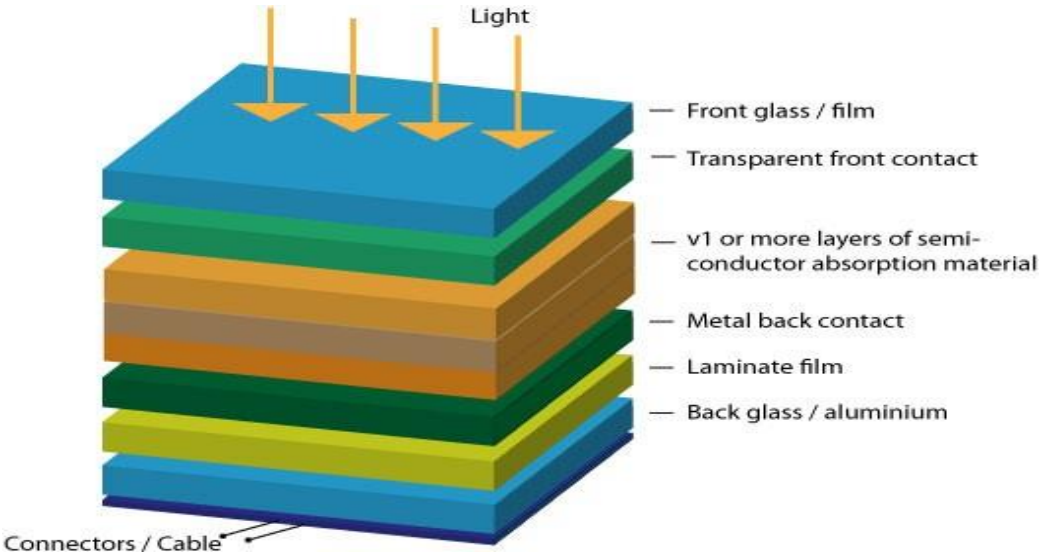

Figure 3.10. the layers of a solar module [64].

Photovoltaic had electrically connected in series and/or parallel circuits to output high voltage, current and power [64].

3.5. A PHOTOVOLTAIC ARRAY

It a complete electricity generation unit consisting of photovoltaic generator in Figure

3.10; Figure 3.11 unlimited modules and photovoltaic [65].

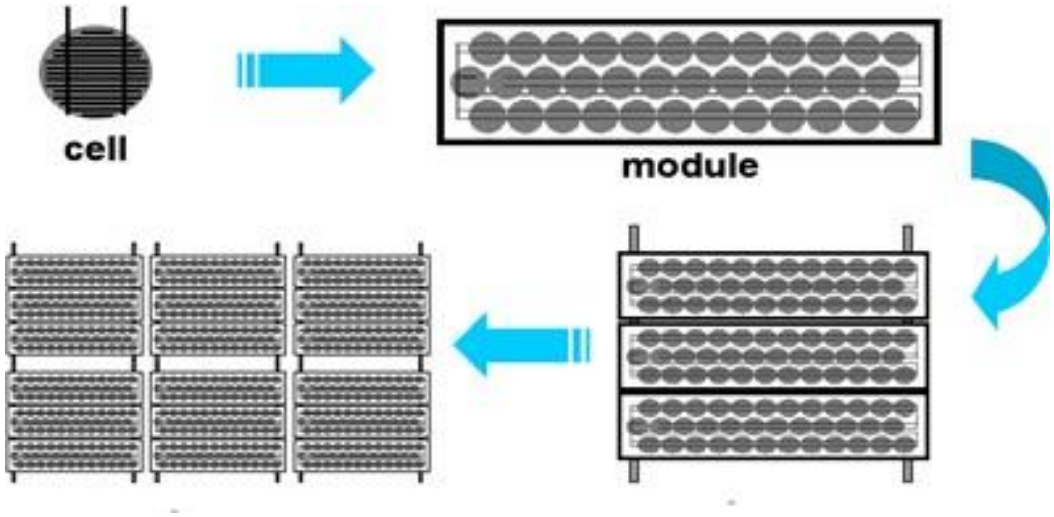

Figure 3.11. Photovoltaic cells, modules, panels and arrays.

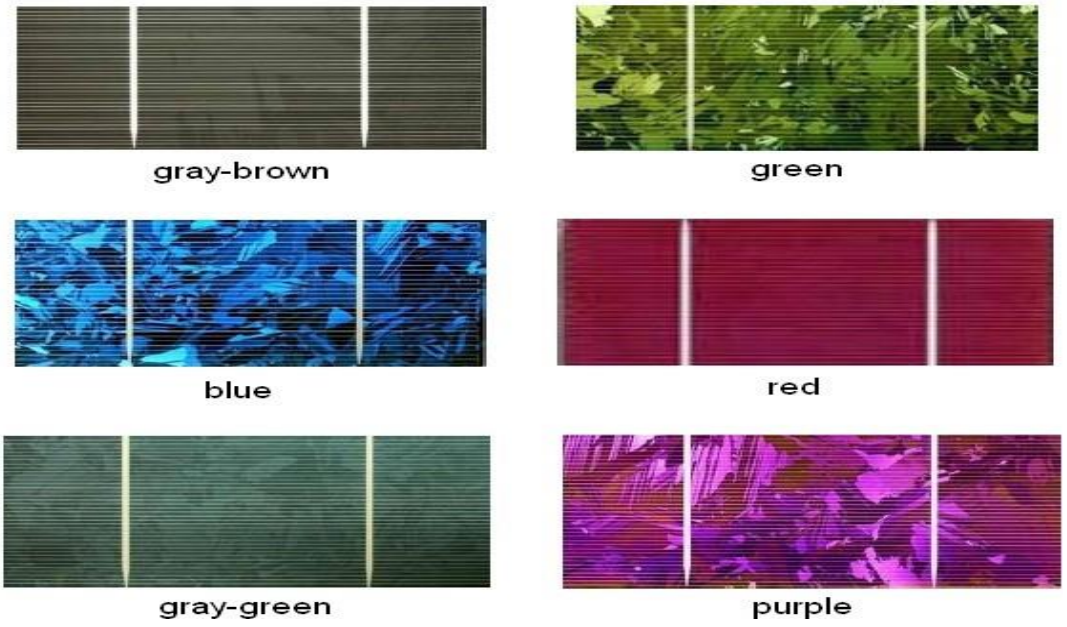

Figure 3.12. Deferent color of PV cell / panel.

3.6. STANDARD TEST CONDITIONS (STC)

Rated maximum DC power output according to Standard Test Conditions (STC). The standard test conditions determined by the unit, which is the cell, as well as the operating temperature. It ranges around 25°C and the solar radiation level is within 1000 watts / m2 and below the air mass spectral distribution of 1.5. In addition, due to the lack of typical conditions for the work of the PV modules and arrays in the field, the actual performance is usually 85 to 90 percent of the STC rating [66].

3.7. SOLAR ARRAY PARAMETERS

- VOC: The maximum voltage supplied by the pattern when the station do not joint to any load. This value is much higher than V_{max} due to the operation of the photovoltaic generator settled by the load. This value count on the number of PV panels linked in series.
- ISC: The maximum current provided by the PV generator when the product conductors are short-circuited. This indicates that the operating current is normal for the circuit.
- P_{max}: is the point where the power is provided through the matrix that is connected
- To the load (batteries, inverters) at its maximum value, Figure 3.13.

Where: Pmax = Imax x Vmax. Maximum power of the PV array point measured in watts (W) or peak watts (Wp) FF: This is the ratio of the maximum power point divided by the open circuit voltage (Voc) and the short circuit current (Isc).
Typical values are between 0.7 and 0.8.

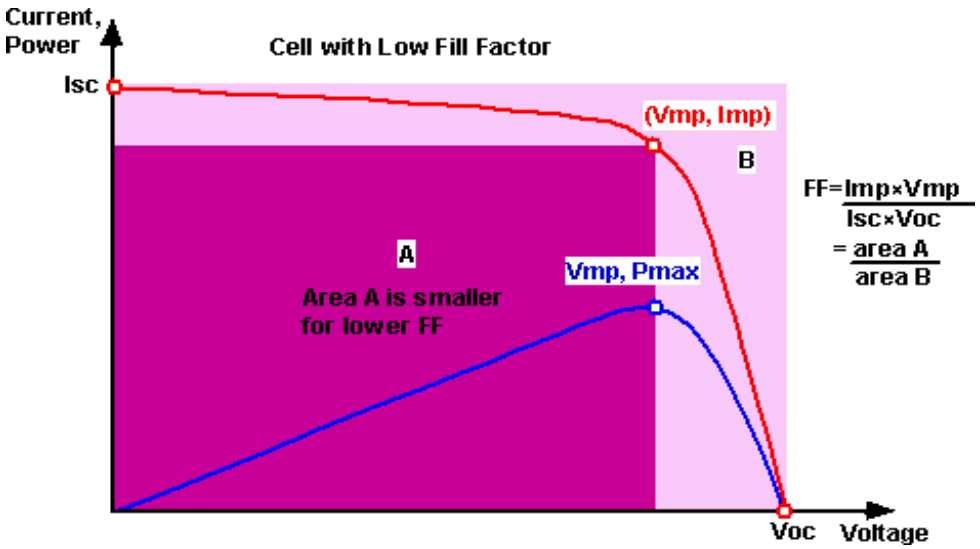

Figure 3.13. The fill factor.

The sort of cell used (amorphous, polycrystalline, monocrystalline, or thin) has a low to approximate efficiency of a typical solar panel. 10-12%.

Knowledge designers who need to configure systems capable of operating as quickly as possible to provide PV I-V curves at the peak power point. [67].

$$\eta_{\max} = \frac{P_{\max}}{P_{in}} = \frac{V_{oc}\, I_{sc}\, FF}{P_{in}} \tag{3.8}$$

3.8. SOLAR SYSTEM OFF GRID

Designed systems to operate all electrical charges for one day. As such, they typically require large battery and solar panel arrays. They may also have wind turbines and, if a creek flows across the property, a micro hydro generator. By their very nature, they have power during all emergencies [68].

3.9. MAIN COMPONENTS OF THE PV SYSTEM

Photovoltaic systems contain a large amount of support equipment in addition to solar units and used to balance the system and make it operate in a sustainable manner. Plugins that vary by size and application include wires, controllers, power storage devices, trackers, mounting devices, inverters, and network connections.

The energy in the solar power plant is flowing during a set of devices, who's joint to a wired web. It often indicates to as System equilibrium (BOS).

The precision of the BOS manufacture had positively reflected in its durable and efficient operation [69].

The general system diagram below Figure 3.14 illustrates some of the main components of BOS.

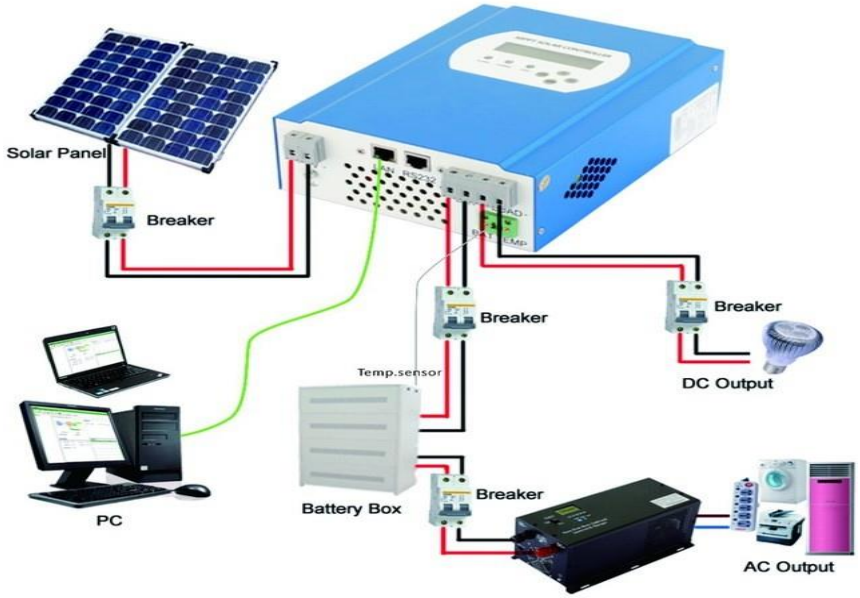

Figure 3.14. Off-grid connected PV system with SCADA system.

We explain the components included in this main diagram as well as their functions:

3.9.1. Charge Controllers

Managing the energy flow between solar panels and storing energy and loads. A system flow diagram controls the charging of batteries as well as protecting them from damage and preventing overcharging or overdosing Figure3.15.

One had used for PWM pulse control and the other for MPPT charge controller.

3.9.1.1. PWM Controller

It is a wrench for parts of the solar system with the battery. This is why the system voltage will drop down near the battery voltage Figure3.16.

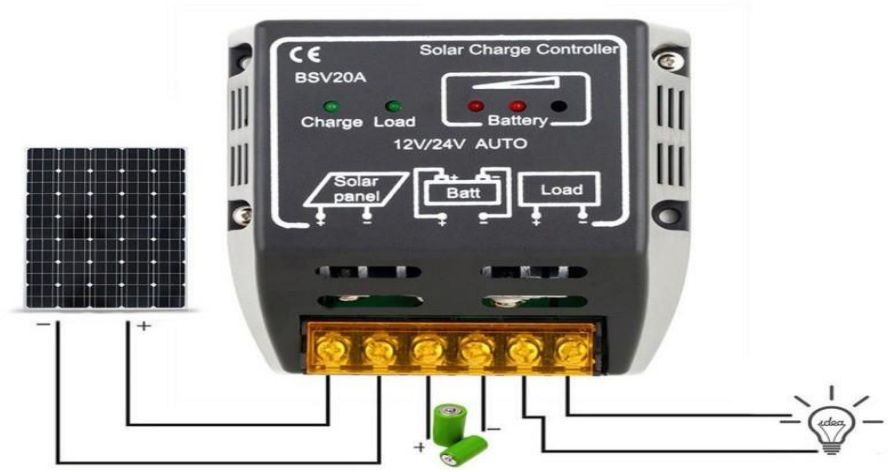

Figure 3.17. PWM charger.

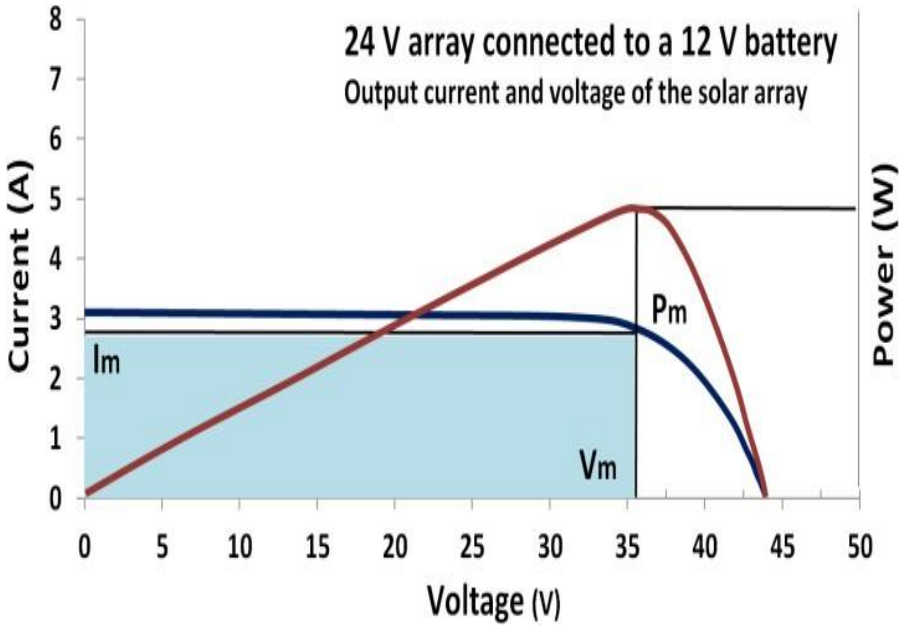

Figure 3.18. PWM controller is a switch connects solar array to battery.

The PWM controller is a switch that connects the solar panel to the battery. When the switch is closed, the voltage of the board and the battery is equal. Take an empty battery and its voltage is about 13 volts. If you lose a voltage of 0.5 volts over the cables in addition to the control unit, the board will be at Vpwm = 13.5 volts.

The higher the battery charge state, the higher the voltage. And for the absorption voltage (14.5V),

The PWM controller then disconnects and reconnects the board to prevent overcharging [70].

In this example, with V_{bat} = 13V and V_{pwm} = V_{bat} +0.5 V = 13.5 V, the power harvested from the panel is V_{pwm} x I_{pwm} = 13.5V × 6A = 81W, which is 19% less than the 100 W.

3.10. MOLDING OF SOLAR PV PANEL SYSTEM ON SITE

3.10.1. Solar Power

$$P_{Design} = G \times A \times \eta_m \times P_R \qquad (3.9)$$

P_D = Theoretical power from solar system (Watts) G = Constant Radiation (W/m²)

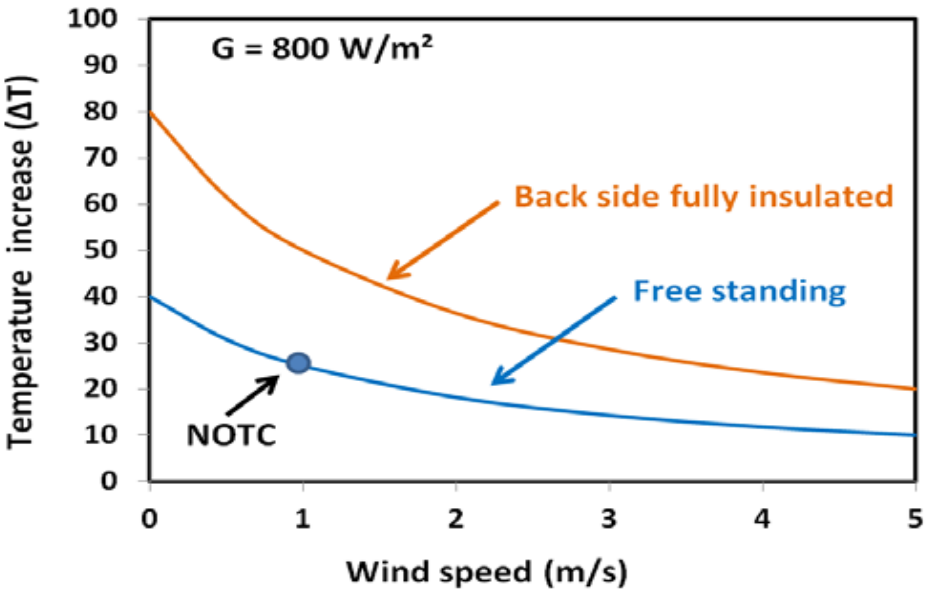

Figure 3.19. Temperature – Wind speed curve.

The equations for the solar radiation and the temperature difference of the system and the surrounding environment show that both the conductivity and the load loss are linear. The temperature does not differ with the thermal resistance and heat transfer coefficient. It had indicated by NOCT for best condition, worst condition and average

PV modules. Aluminum tubes installed at the back of the unit for cooling reduce thermal resistance.

Three scores of significances for NOCT operation were the typical score of 33°C, the worst 58°C and the typical unit at 48°C respectively Figure3 20. It is calculated as follows: [71].

$$T_{cell} = T_{amb} + (NOCT - 20/80) \bullet S \qquad (3.10)$$

T_{cell} = Panel temperature model °C.

T_{amb} = Air temperature °C

NOCT = Normal operation cell temperature (47°C).

S = insolation in m W/cm^2.

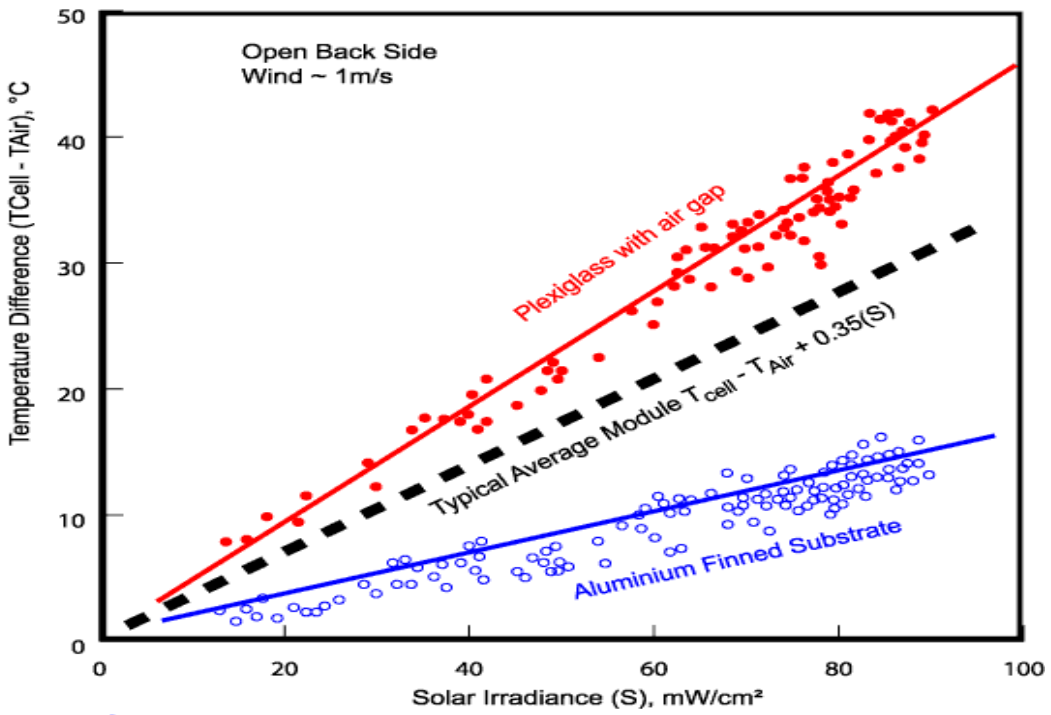

Figure 3.21. The different module types.

$$P_{SITE} = I_m \times V_m \qquad (3.11)$$

P_{site} = Measured Power from Solar system, I_m and V_{oc} measured Values at site.
Note: V_m = Max. Voltage. (V_{MPP} = k x V_{oc}) k_1 = 0.71 - 0.78.
I_m = Max. Current. ($I_{MPP} = K_2 I_{OC}$) K2 = 0.78 - 0.92[4].

3.10.2. Power Out Put

All photovoltaic modules tested by STC, which is the standard test that meets all laboratory conditions. STC means Figure 3.19:

- 1000 w/m^2: An radiation.
- 25°C: surface temperature.
- AM 1.5 G: A light spectrum.

3.10.3. The Performance Under NOCT Conditions

The temperature and radiation are usually different from the STC, so high temperatures or low radiation result in low PV capabilities. Note that NOCT conditions are generally less than 18 to 26%. Two mathematical equations had used; first the temperature of the PV cell is determined. T_{cell}: Figure3 22.

$$T_{cell} = T_{enivorment} + 1.25 \times Irradiation \times (T_{NOCT} - 20) \quad (3.12)$$

T_{NOCT} is in the datasheet. We also use an average value of 46°C in the absence of data, and we calculate the PV under NOCT conditions, and the NOCT performance:

$$P_{NOCT} = P_{STC} \times \left[1 + P_{tempcoaf} \times (T_{cell} - 25)\right] \quad (3.13)$$

P_{STC} performs PV under conditions of STC.

$P_{tempcoef}$ is the power temperature coefficient. [72].

Figure 3.23. on site solar PV system.

3.10.4. Second Method for Estimate the Temperature Coefficients

Trina Solar PV module as an example, calculates energy loss when installed in an area with a hot climate. We choose the 60-cell polycrystalline silicon module currently highest power: 260W. The temperature coefficient for maximum output power (Pmax) at STC is -0.41% /°C [73].

3.10.5. PV Module Efficiency

The unit voltage and current depend on the temperature. Therefore, the ambient temperature and the unit temperature affect the efficiency of the PV module. The maximum power of a PV module is [7]:

$$P_{mp} = V_{mp} \times I_{mp} = V_{oc} \times I_{sc} \times FF \qquad (3.13)$$

Pmp: maximum power. Vmp: maximum voltage. Imp: maximum current. FF: fill factor.
Voc: open circuit voltage. Isc: short circuit current.

As the module temperature increases, also I_{sc} rises. The efficiency of a PV cell is the ratio of energy output divided by the energy input provided via the Solar radiation s appear at Eq. (3.13) [74].

$$\eta = \frac{E_{out}}{E_{in}} \tag{3.14}$$

Also the PV module efficiency of Eq. (3.14)

$$\eta = \frac{P_{\max}}{E \times A} \tag{3.15}$$

P_{max} is the maximum power; E is the solar radiation under STC (W/m^2). A is the surface area of the module in m^2. For the efficiency utilize the relation in as [75].

$$\eta_{pv} = \eta rT \left[1 - \beta\left(T_{pv} - T_r T\right)\right] \tag{3.16}$$

η_{pv}: the efficiency of the PV cell. ηrT: the PV module efficiency at the reference temperature (25 C). T_{pv}: the temperature of the PV module cell. β: the temperature coefficient of power and T_rT is the reference temperature of the PV module. [76].

3.10.6. PV module affect by temperature

The effect of the temperature of the PV module could expressed utilized the energy equation of the PV array as in Anon (2014) as:

$$P_{pv} = Y_{pv} \times f_{pv} \left(\frac{G_T}{G_{T,STC}} \right) \left[1 + \alpha_p \left(T_C - T_{C,STC} \right) \right] \qquad (3.17)$$

Y_{pv}: PV array capacity.

F_{pv}: the photoelectric power reduction factor (%).

G_T: the solar radiation incident on the PV array at the current time step (KW / m2).

$G_{T, STC}$: the incident radiation at standard test conditions (1 KW / m2).

α_p: the power temperature coefficient (% / C).

T_c: the temperature of the photovoltaic cell in the current time step (C).

TC, STC is the temperature of the photovoltaic cell under standard test conditions (25°C).

The power temperature coefficient of the PV module is fundamental, because it helps in limit the deviation of the power generated via the module of; the power temperature coefficient of this PV module is −0.44%/C. Otherwise, the test calculates the factor of reducing the value of the PV module; this is because the PV modules, measured in the field, may mark that the unit powers obtained are different from those of the nameplate readability.

Environmental factors that reduce the efficiency of a photovoltaic module include clouds, high dust concentration and shade. Implementing a PV unit experiment with a derivation factor of 0.95 indicates that the test produced power readings in STC, which is 5% lower than the manufacturer's nameplate rating PV. The power output equation uses the PV panels to consider factors such as wire loss, shading, and others.

Derivation factor 0.8 to calculate losses and dispersion factor 1.0 for fixation that is in an ideal position. The efficiency of the PV panels can expressed as [77].

$$\eta_{mp,STC} = \frac{Y_{pv}}{\left(A_{pv} \times G_{T,STC}\right)} \qquad (3.18)$$

Where $\eta_{mp,\ STC}$ is the efficiency PV modules under standard test condition (%).

Ypv Represents the PV module's rated power output at STC (KW), Apv Is the PV module's surface area (m^2), GT, STC Represents the radiation at STC (1 KW/m^2).

By substituting, for Apv. $\eta_{mp,\ STC}$ = Ypv/ (Apv × $G_{T,\ STC}$), in Eq. (5), the efficiency of a PV module becomes [78]:

$$\eta_{mp} = \frac{Y_{pv}}{A_{pv} \times G_{T,STC}} \qquad (3.19)$$

$\eta_{mp,\ STC}$ = the efficiency of the PV module under standard test conditions [%]

Y_{PV} = the rated power output of the PV module under standard test conditions [kW]

A_{PV} = the surface area of the PV module [m2]

$G_{T,\ STC}$= the radiation at standard test conditions [1 kW/m2]

3.10.7. Photovoltaic module temperature

This parameter shows how the PV cell temperature affects the energy generated by the model. The value of the temperature coefficient is negative in order to increase the temperature of the photoelectric cell, with lower energy output. The temperature

coefficient of the 150 W PV module model used in these tests is −0.44 % reduction. When the temperature increases above 25ºC, the power output reduces and when the temperature of the module surface reduces below 25ºC, power output increases [72].

CHAPTER 4

SYSTEMS DESIGN AND METHODS

4.1. EXPERIMENTAL DESIGN, SETUP AND PROCEDURE

Two types of efficiencies have been worked out in this test system: these are thermal and electrical efficiencies. For the electrical and thermal efficiency of photovoltaic panels, it is observed that when the photovoltaic panels convert the incoming solar radiation into thermal and electrical energy, the efficiency decreases. It is possible to produce thermal energy by taking advantage of the heating feature of these PV panels. These systems are called photoelectric and thermal systems in the literature. The special treatment on the PV module has been carried out in many experimental studies. Since studies are requiring special handling on the unit, this is still just stay as laboratory work. In this study, different PV / T systems of photovoltaic modules for cooling were analyzed experimentally. A simple tube installed in the PV module as a spiral heat exchanger to provide active cooling. The model easily applied to large-scale systems.

In Figure 4.1 and Figure 4.2 has shown the design of the experiment parts, which is the same as proposed in this thesis. The PV and PVT panels are change as follows:

- A concentrator was used in the system for concentrating solar radiation as seen in Figure 4.2.
- For PV, the studies were done due to;
  PV1 panel with sheet and tube- serpentine type:

A 20-watt PV panel of 640×300×28 mm attached to absorber copper plate as a Serpentine Shape as seen in Figure 4.3

PV2 panel with sheet and tube – serpentine type:

A 10-watt PV panel of 340*235*17 mm attached to absorber copper plate as a Serpentine shape as shown in Figure 4.2.

In addition, the backside PV the plate was covered with spiral copper pipes (see Figure 4.2.).

The experimental system has been tested using the following variations.

- The model without using the fluid.
- The model using water.
- Bring the fluids

Figure 4.1. Manufactured of concentrated solar air collector with heat store.

4.1.1. Experimental Setup Configures Ration and Compounds

In Figure 4.2 and in Figure 4.3 has shown that he design of the experiment parts, which is the same as proposed in this thesis, but the PV and PVT panels, are change as follows:

- A concentrator (Number 1 in Figure 4.2) was used in the system for concentrating solar radiation see Figure 4.3.
- PV, PV1 panel with sheet and tube- serpentine type:
- A 20-watt PV panel of 640×300×28 mm attached to absorber copper plate as a serpentine Shape (see Figure 4.2)
- PV2 panel with sheet and tube – serpentine type:

A 10-watt PV panel of 340×235×17 mm attached to absorber copper plate as a serpentine shape Figure 4.2.

In addition, the back PV the plate was covered with spiral copper pipes (see Figure 4.4.)

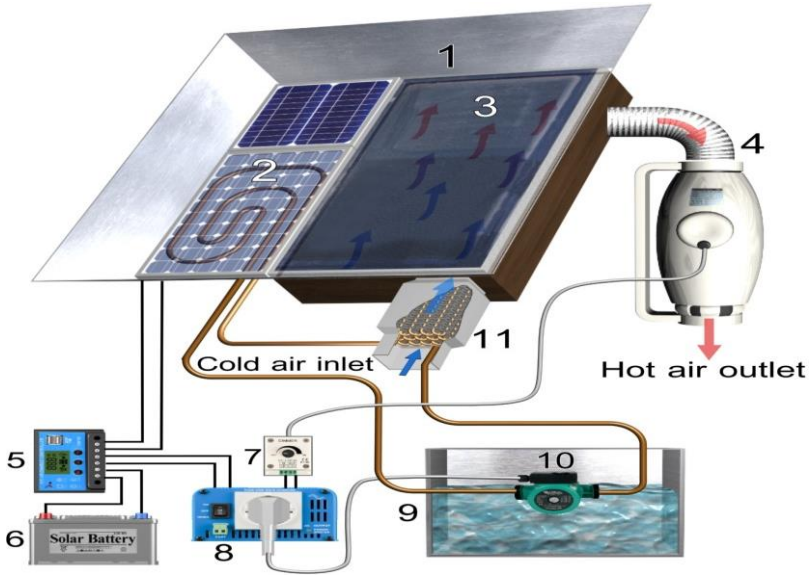

1. Concentrator, 2. PV module, 3. Air collector with paraffin wax, 4. Fan, 5. Charge controller, 6. Solar battery, 7. Fan speed controller, 8. Inverter, 9. Depot, 10. Pump, 11. Heat exchanger and cold air inlet to the air collector.

Figure 4.2. The flow diagram of the CPV/T system Operating procedure.

- Concentrate (Solar radiation was concentrated on air collector and PV modules; it aimed to increase the electrical and thermal gains obtained from PV modules).
- PV modules
- Solar air collector as shown in Figure 4.3. Exploded view of the designed air collector.
- The fan has a role in increasing the current in the system and is a controller in terms of speed (No.4 in Figure 4.2). The fan provides the system with the necessary energy by increasing the speed of the air during the solar surface period. When solar radiation is not sufficient, the fan generates power from the battery. The machine diagram has shown in Figure 4.2
- The charge controller, which is a 10 Amp capacity, is controlling charging and discharging process of the battery bank. The controller main mission is to prevent overcharging and to protect the battery bank from overvoltage, which may reduce battery performance or life.
- Solar battery, which is the main unit, is responsible for storing energy in the system during the daytime. A connected solar system charge it. Electricity stored is consuming after sunset, during peak power demand, or during a power outage.
- Fan speed controller which is a part of fan Control Unit is an important section that increases or decreases fan speed according to your requirements.
- The inverter is an electrical device or a circuit that changes direct current (DC) of the Battery Bank or solar PV panels to alternating current (AC).
- Depot a place for the storage of fluids.
- The rotary pump is a positive displacement pump. With each pump cycle, a steady volume of liquid is moved regardless of the resistance of the pump.
- The heat exchanger, the heat exchanger is used to change the temperature of a fluid by passing through the tubes and other medium. The other medium usually has higher temperature, it causes to raise the temperature of the fluid. The fluid can also be cooled when pass through the tubes in the middle of low temperature media.

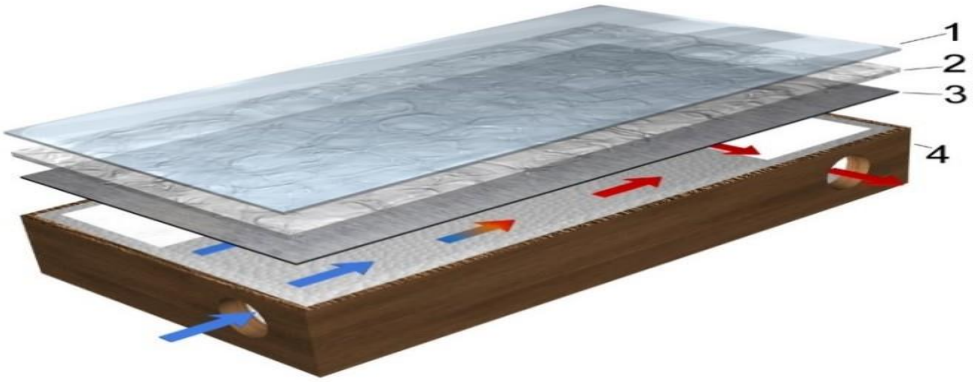

1. Glass, **2.** Microcrystalline paraffin wax, **3.** Aluminum plate, **4.** Collector case

Figure 4.3. Exploded view of the designed air collector.

Low temperature applications in our proposed model, and heat transferred from the photoelectric system to fluids was used to heat the air entering the air pool using crystalline paraffin. In this way, the system performance should be increased by providing heat storage using the distinct features of PCM and heating the outside air entering the collector. The system was used in the winter months when in need to heating energy. On days when sunlight and room temperature are sufficient, the fine crystalline paraffin wax used in the air collector increases the effect of the condenser.

4.1.2. Fluids use for Cooling

The experimentally investigated CPV / T was tested using 3 different fluids. The used fluids has been shown in Table 4.1. The fluids tested in the system by passing through spiral pipes has been shown in Figure 4.4. Copper pipes in Figure 4.4 cover the back of the PV / T system.

Table 4.1. Fluids Used İn This Study (Property Tables and Charts (Sı Units)).

Fluid	Specific Heat $J \cdot kg^{-1} \cdot K^{-1}$	Density kg/m^3
Water	4.18	998.49
White Spirit	2.43	790
Ethyl alcohol	2.3	789

Figure 4.4. the front and rear view of the CPV/T system.

4.2. DESCRIPTION OF THE DEVISES AND EQUIPMENT

We used several devices in our experiments that helped us to obtain an effective result (shown in Table 4.2, 4.3).

Table 4.2. the properties of used equipment.

Equipment Name	Capacity	Q.T. Y	Equations
Inverter	100 W	1	3
Solar Charge controller SCS	2 A	1	2
Battery 12V	100 W	1	3-4
Solar Battery	30 Ah	2	5
Fan	25 W	1	-
Solar panel	20W	**1**	**6**
Solar panel	10W	**1**	**6**

Table 4.3. Description of devices and control equipment.

Equipment	Properties
Solar Meter to measure the global solar irradiation.	Model-130 1500 W/m^2, sensitivity ±1.5%
Anemometer.	Sensors K-types, RTD and PT100 thermocouple, and Hg thermometer
Seven thermocouples.	DIN 43710 and IEC 584
Fan TD-SILENT SERIES	(TD-250/100 SILENT (230-240V 50/60)).
Solar Control Charger.	MEXXSUN 10 AMPER MPPT
Dimmer.	DC 12-24V 8A.
Data logger with 15 channels.	Model DI-808 (Built-in Web Server for Io T Applications)
Multi meter	Digital multimeter-UT71C/D/E
Flow meter	Rotameter-LZB10
Circulation Pump	ACe220 Ve13W
Tank	5Lit
Paraffin wax Cn H2n+2	Cn H2n+ D2

4.2.1. Inverter Calculation

Inverter power must not be lower than that of the equipment running simultaneously. Calculated inverter size based on its equality to 1.3 larger than load power.

4.2.2. Charge Regulator Calculation

$$I_{cc} = \frac{RP}{V_m} \square 30\% \qquad (4.2)$$

Where Isc is the short circuits current

4.2.3. Data Acquisition System

Fabricated Figure.4.5, which has 18 channels for temperature measurement, is channelized for measuring current, voltage, and solar radiation.

Figure 4.5. Data acquisition system.

4.3. SERPENTINE HEAT EXCHANGER DESIGN

Serpentine Figures 4.6 which is heat exchangers are constructed in the energy laboratory. In addition, It is making control for leak in the entire pipe system.

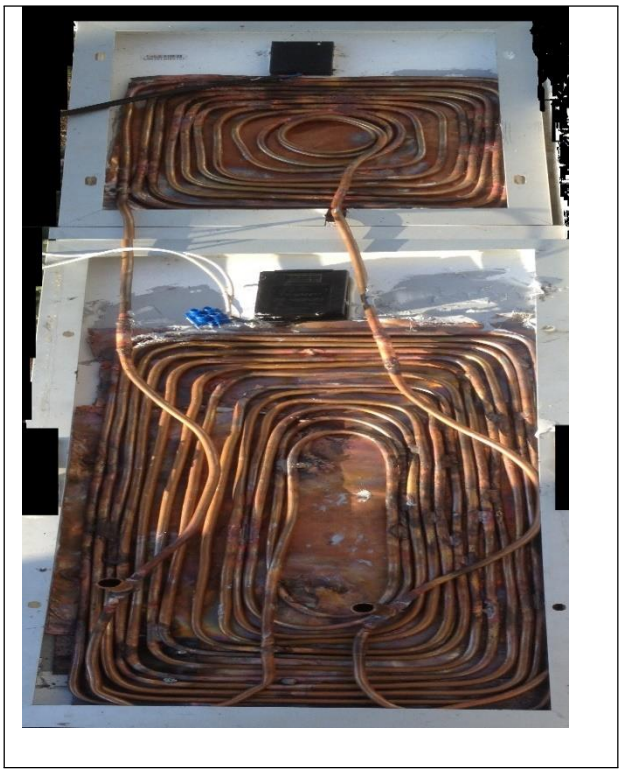

4.4 Figure 4.6. Schematic diagram for serpentine heat exchanger design.

There are some steps which have been considered before running the experiment:

- All the sensors and transducers must have calibrated before and after mounting in the test rig.
- All Environmental conditions (i.e., being in the environment) such as air, solar radiation, and air velocity have to be considered. The test have to be conducted in the midday sun on clear days.
- The flow rates for the working fluid must calculated based on the meteorological data recorded for the city of Karabuk. Turkey of the solar radiation and the ambient temperature on site, as well as the specifications for the PVT model are the considered variables.
- The experiment have to be carried out for pure water and white spirit, ethyl alcohol with different concentrations. Set the specified flow rate by adjusting the control valves. If the pump has variable flow rates; change flow rate and the

pump lead the rate regulators.

- Once the flow rate (mf*)* is set, the working fluid outlet temperature (T_{fo}) can b e measured at a constant working fluid inlet temperature (T_{fi}), solar radiation (I_t) and ambient temperature (T_a).
- During this period all other parameters such as, cell surface temperature for PV and PVT (T_{pv}, T_{pvt}), the output voltage and current for systems, and storage tank temperatures can be measured to get a measuring points.
- In order to obtain more measurement points, we are changing each the fluid test, as well as the fluid flow rate and increasing the fan speed.

4.5. RESULTS ANALYSIS METHODS

To test the effects of using the prepared liquid as a working fluid in the PVT system, the experiment results should have analyzed and discussed to conclude the the following issues:

The temperature profile of PV cell, PVT cell and collector outlet during the day for pure water and different concentrations of fluid are tested. This shows the effect of PV cells cooling and thermal efficiency yield of PVT collector.

The electrical output, thermal gain and the performance of PVT with pure water and liquid compared to PV efficiency are also tested. This illustrates the effect of photoelectric cooling on energy-saving PV.

4.6. OPERATING PROCEDURE

Flowchart of the control system given in Figure 4.8. The normal fluids (water, alcohol, or ethyl alcohol) flowing from the depot by pump push the liquid through the flow rate to system PV at the point (T4) are also given in Figure 4.7. Then the fluids pass through a transparent spiral cooling tube exits at the point (T5). After that the heat exchanger

is followed and it returns the depot. Dimmer controls it. The system works as follows:

- The hot air comes to the solar collector the point (T1) point through heat exchanger and comes out at point (T2).
- Liquids enter the designed model via T4 and then exit via T5.
- Normal air from the T6 point enters the heat exchanger and then passes into the collector from T1 point.
- The ambient air temperature is calculated by T3 attached to a data acquisition system.
- The thermocouple has been fixed behind the solar panels so that the heat has to be calculated by the T7 attached to a data acquisition system.
- The heated fluid exits the solar panels via T5 to the heat exchanger.
- In this model, both the air and the fluid cool the solar panels, which shows the
- Harmony between them. This has been done via a heat exchanger.

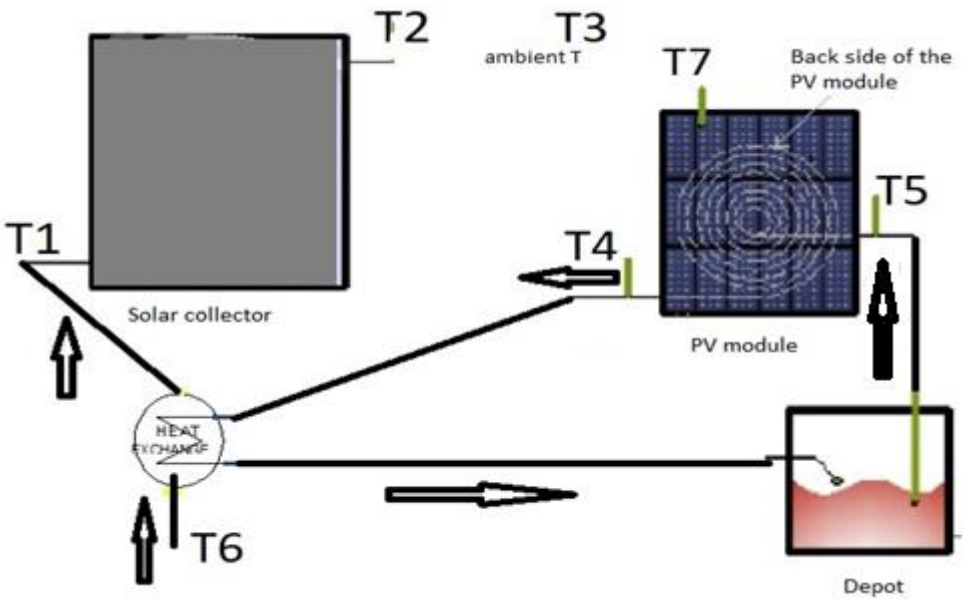

T1: SC IN, HE OUT. T2: SCOUT. T3: Ambient. T4: PV IN. T5: PV OUT.T6: HE IN.

Figure 4.7. Designed PV and thermal system.

4.7. ANALYSIS OF THE ENERGY SYSTEM

It becomes clear to determine the relationship between thermal efficiency of the PV module and the solar collector. In mathematical equations, the relationship between these factors had explained by analysis and concluded with the below given formula. The useful rate of thermal energy gain, which obtained from the solar collector, can be determined as the follows:

$$Q_{u,sc} = m_{air} \times C_{p\,air} \times (T_{o,sc} - T_{i,sc}) \tag{4.3}$$

Whereas, Qu the useful energy transfer rate and its unit (W), ṁ mass well as the mass flow rate of megawatts (kg / s), Cp heat of the specified air (J/(kg K)), temperature T (°C), solar collector.

The thermal efficiency of the collector can have computed using solar energy into useful thermal values of a sensor and a sensor surface solar radiation.

$$\eta_{th,sc} = Q_{u,sc} / (A_{sc} \times It) \tag{4.4}$$

η_{th}, efficiency of solar cell, It solar intensity (W/m^2).

From this module, according to the use of thermal energy transfer, the circulation process of the water cooling of the PV module will have been calculated as the following:

$$Q_{u,m} = m_w \times C_{pw} \times \left(T_{o,m} - T_{i,m}\right) \tag{4.5}$$

The equation for entering and leaving water temperature is the spiral leg Ti. The thermal efficiency of the circulation water of the PV module can be calculated as follows:

$$\overset{g}{\eta}_{th,m}=Q_{u,m}/(A_m \times I(t)) \qquad (4.6)$$

In the equation (4.6), A_m is the total surface area of the module and I(t) is the amount of solar radiation. Analyses of the electrical efficiency of the PV panels must be done in two categories, first one as the module efficiency and the second one as the cell efficiency.

Am variable in the equation is the sum of the unit, and I(t) is the area of the amount of solar radiation. That is the case with the electrical photovoltaic overlaid the boards with two kinds of efficiency: the lodge of the unity and electricity efficiency, to maintain.

It is necessary to analyze the electrical efficiency of the photovoltaic panels in two categories as module and cell efficiency. The biggest electrical loss of the panels occurs with the temperature. Open circuit voltage and fill factor decreases significantly with temperature. Nonetheless, short circuit current increases for a while [1, 7]. At the end of this common effect, electrical efficiency calculated as:

$$\eta_C = \eta_0 \left[1-\beta(T_C-25)\right] \qquad (4.7)$$

Where ή0 is the efficiency as Standard Test Conditions, STC (It = 1000 W/m^2, Tc=

25°C), T_C is the solar cell temperature and β is the electrical efficiency thermal coefficient. β value is dependent strongly with the type, characterizes of the materials from which solar PV module is produce.

For a siliceous nature of the crystalline material, it is almost taken as 0.0045/K. Usually, the solar PV module electrical performance gives in unit grams and do the following:

$$\eta_m = \eta_C \times \tau_g \times \alpha_C \times \delta_C \qquad (4.8)$$

Where τ_g is the transparency range for the solar PV module glass, άc is the absorptivity of the solar PV cell and δ_c is known as packing factor ranged between (0.90, 0.95 and 0.90). Another expression of the effectiveness of a parameter is as follows:

$$\eta_m = P/(A_m \cdot I(t)) \qquad (4.9)$$

The output power P of the PV from the skirt using a large voltage and current values are measured as follows:

$$P = V \times I \qquad (4.10)$$

This gain calculated from PV of electrical energy is obtained as:

$$E_{nonelectrical} = \eta_m \times A_m \times I(t) \qquad (4.11)$$

Where η_m is the module efficiency, A_m is the module surface area.
Energy of solar PV module consist of two types which are thermal and electrical. The process of the thermal energy gain can be explained by converting electrical energy to

thermal energy. At the same time, thermal energy can be added to the overall system gain as follows [79]:

$$Q_{u,overall} = Q_{u,m} + Q_{u,sc} + \left(\frac{E_{1,electrical}}{C_{power}}\right) \quad (4.12)$$

Where C_{power} is the conversion factor of the thermal power plant depending on the quality of the coal (0.38). This value is between 0.20 and 0.40 [1]. The total efficiency assurance cannot be guaranteed:

$$\eta_{overall} = Q_{u,overall} / [(A_m \times I(t)) + (A_{sc} \times I(t))] \quad (4.13)$$

The powers of the solar PV modules obtained at the Standard Test Conditions STC can be called as the high limit because the solar radiation is 1000W/m^2 and the ambient temperature is 25^{O}C. Therefore, the divisibility of the power obtained at the standard test conditions to power obtained on our site environment conditions could be defined as an "availability" and expressed as follows:

$$\eta_{avail} = \frac{P_m}{PT} \quad (4.14)$$

CHAPTER 5

DISCUSSION

The PVT system tested in the first step can be categorized as follows; the experiment carried without cooling, second cooling with only water and third cooling with sprit liquid. The tests are aiming to compare the performance of the system under these three tests.

5.1. PV/T ANALYSIS SYSTEM WITHOUT COOLING

Field measurements of solar radiation–Efficiency curve during 8h from 9:00 – 17:00 has been shown in figure 5.1. The solar radiation and efficiency range is changing between 0-14.1ºC and 190 -1000 W/m^2.

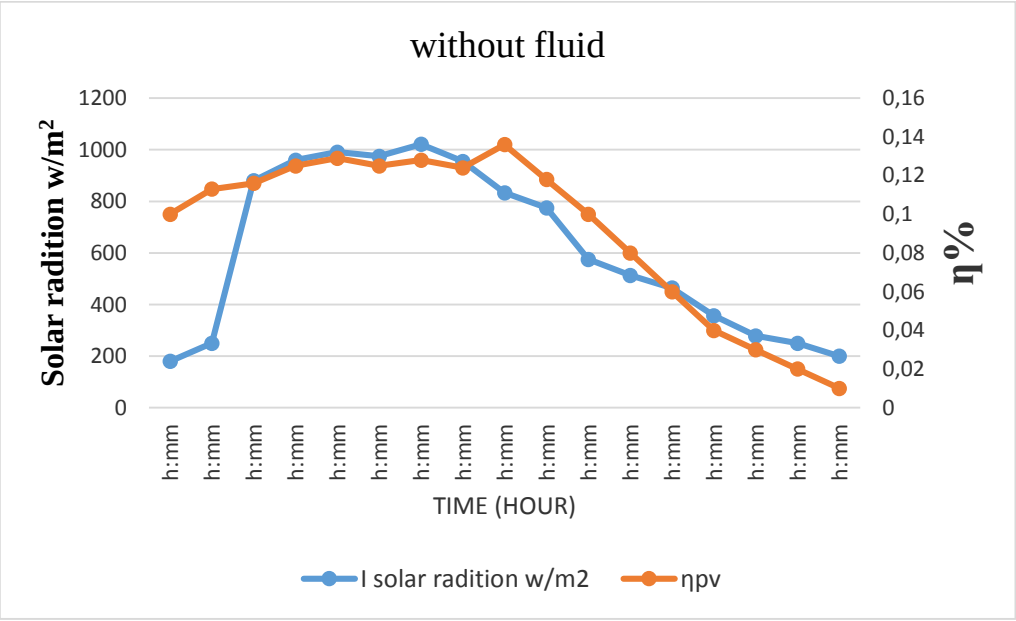

Figure 5.1. Solar radiation and PV efficiency a cording to time.

In this experiment water is divided into the test period for two regions, the first region from 9-12:30 in which the radiation average increased for 190 W/m^2 until 1000 W/m^2 was observed. It must be big, and it ranges its efficiency between 0.01 % - 0.13%. The second region from 12:30 – 17:00, the radiation range is changing 1000-190 W/m^2, and the Efficiency range is 0.13%- 0.01%.

In Table 5.1 the result of experiment without fluid, when Solar radiation 600 W/m^2 in the air temperature surrounding with a value of 7.2, are given. The average temperature for SC inlet and outlet without fluid is 2ºC. Moreover, the efficiency for PV module is 19%.

Table 5.1. System without cooling Results Analysis.

PVT module and solar collector process		Descrbe
Average	ambient temperature (ºC)	7.2
	Solar radiation W/m^2	600
	temperature for SC inlet (ºC)	25
	temperature for SC output (ºC)	27
	PV Actual power P = IV (W)	25
	PV Design power E (W)	30
	The efficiency for PV module without cooling (%)	19
Fan speed (m/s)		1
Solar Panel Current (A)		0.8
Solar panel voltage (V)		19.6

5.2. PV/T SYSTEM ANALYSIS COOLING BY WHITE SPIRIT WITH THERMAL ENERGY DEPOT

5.2.1. Solar Radiation

Solar meter is recording between 9:00 and 17:00 with an interval of 30 minutes in each day as shown in Figure 5.2. At sunrise in the morning, solar radiation reaches its maximum value. There is a change in the radiation. However, when the sun falls, the radiation gradually decreases.

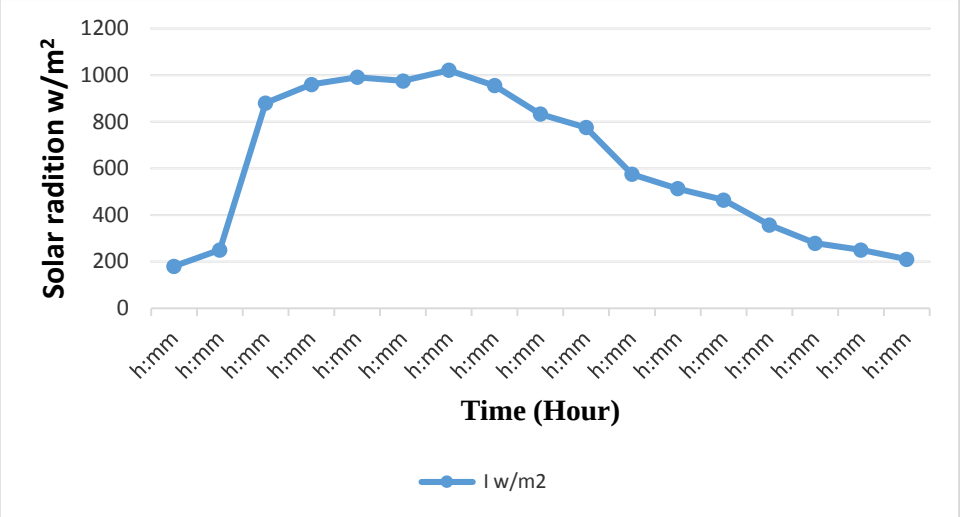

Figure 5.2. The variation in concentrated solar radiation.

The first graph in Figure 5.3 shows the ambient and outlet air temperatures of the system without the heat storage unit.

It is concluded that when the outlet air temperature had been -10°C, the supply air temperature of the concentrating air collector without the heat storage unit had reached above 45°C.

After the system filled with microcrystalline paraffin wax as the heat storage material, it analyzed experimentally for four days. The solar radiation data for the system with the paraffin wax has been shown in Figure 5.3

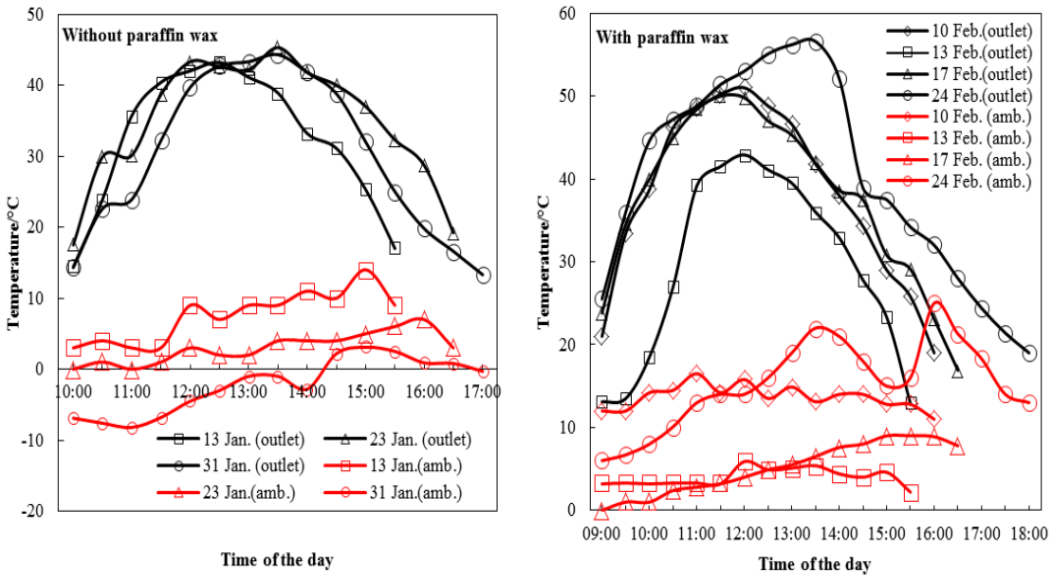

Figure 5.3. Solar collector outlet temperature and ambient temperature differences according to experimental time.

5.2.2. Electrical Energy

The electrical energy obtained in the gain PV module were estimated by using Eq. (4.11) and given in Figure 5.4. The value radiation is max 1021 W/m^2 and minim 250 w/m^2. The average value is 702w/m^2 while the max. Power is 37.4 W and the minimum is 27.5 W with average value 30.2 W, from Figure. 5.4 We can see the radiation above 1000 W/m^2, In this case, the efficiency of the PV system has decreased and the electrical energy gain has increased.

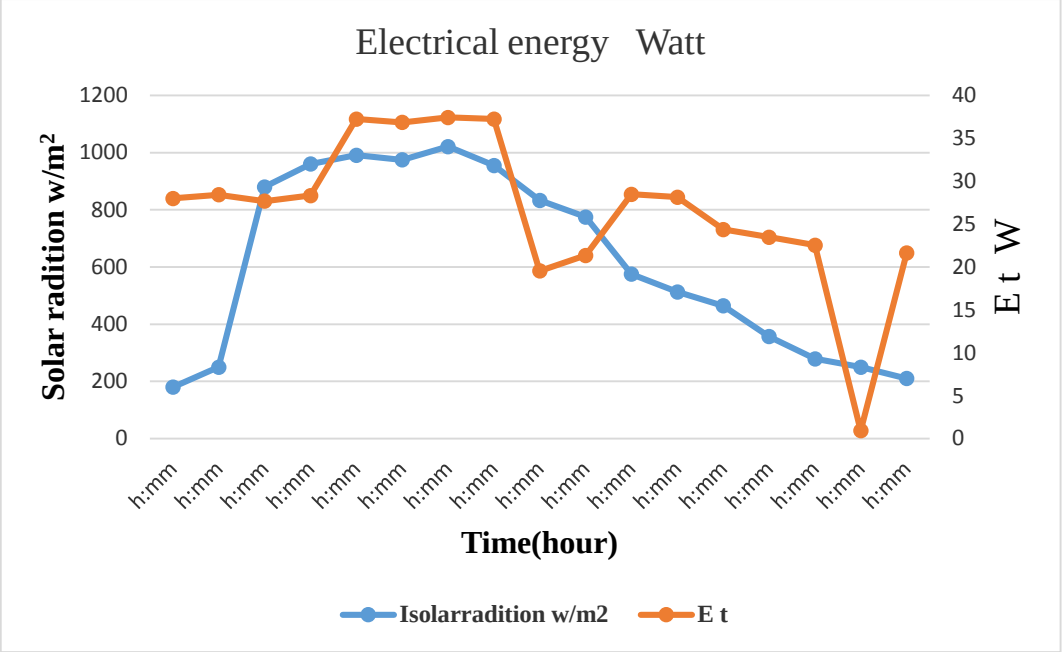

Figure 5.4. Solar radiation and electrical energy gain differences according to experimental time.

5.2.3. Actual Power

The power module Eq. (4.10) current and voltage measurement has been estimated. In addition, compared with Eq. (3.8) Figure 5.6, the relationship between current and voltage in the experiment has been determined. The power of the module (Eq. 4.10, Figure 5.5) change in parallel solar radiation is given below with the increasing in power and solar radiation.

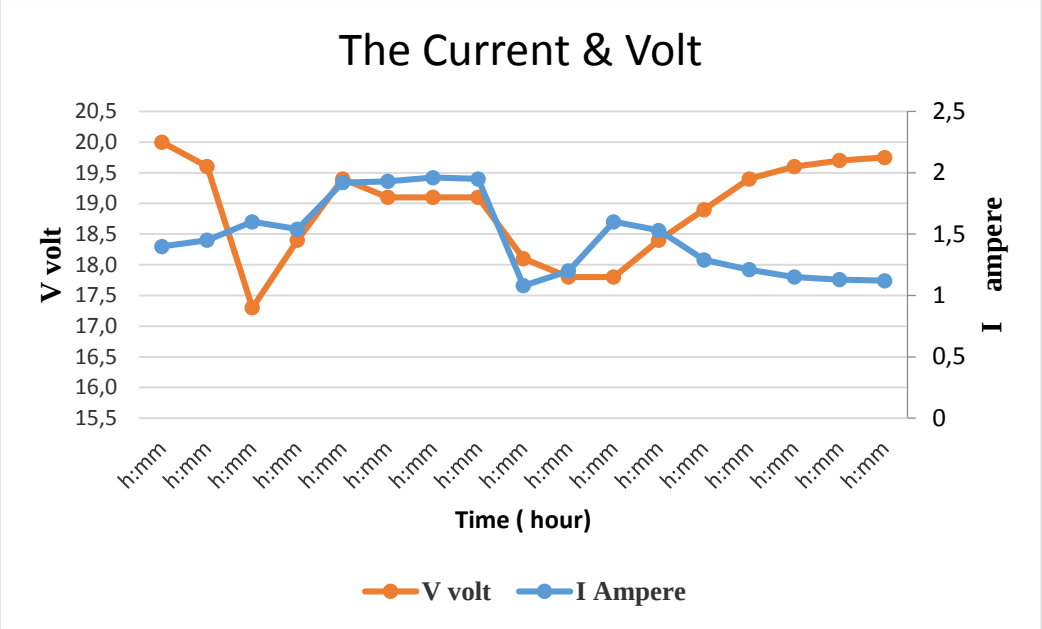

Figure 5.5. V&I Curve.

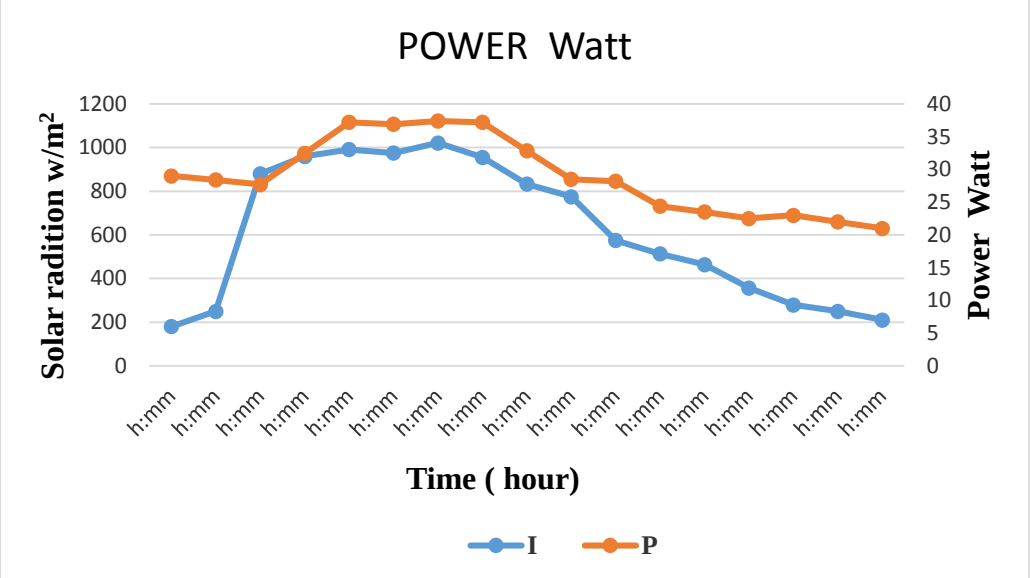

Figure 5.6. Solar radiation – Power curve.

5.2.4. Efficiency

The efficiency of the PV/T system without cooling was 13%, and the efficiency of the

cooled photovoltaic was between 14% and 26% Fig 5.7. According to the figure, as the solar radiation increases, the efficiency of the PV system has been decreased. Therefore, efficiency alone is not an important indicator for solar PV systems.

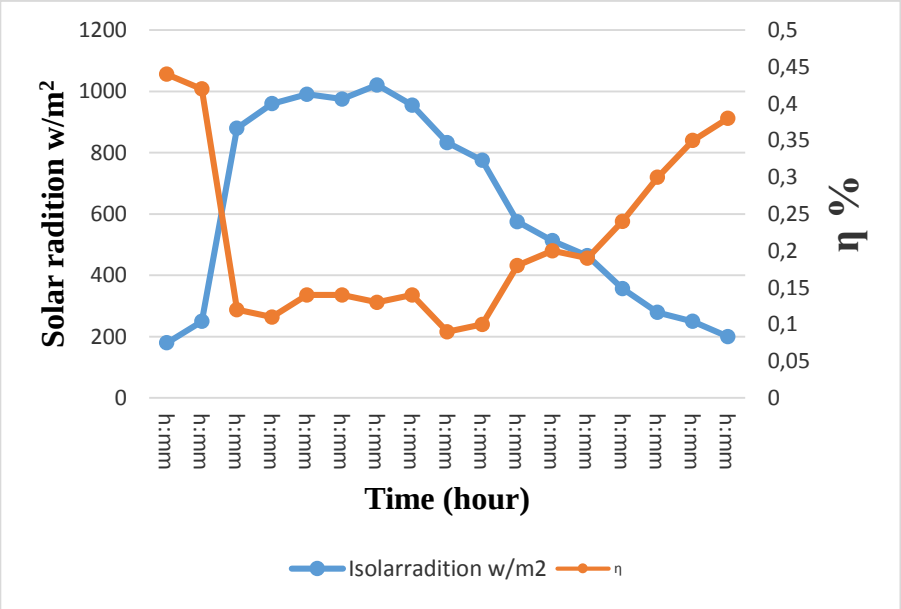

Figure 5.7. The efficiency with cooling.

5.2.5. Thermal Energy Gains

In equation (4.12) and Figure 5.19, during the experiments the solar radiation on the PV module and the air collector reached to the value of 1000 W/m² with the designed concentrator. The average solar radiation on the system was 600 W/m². The temperature collector outlet reached up to 35 °C.

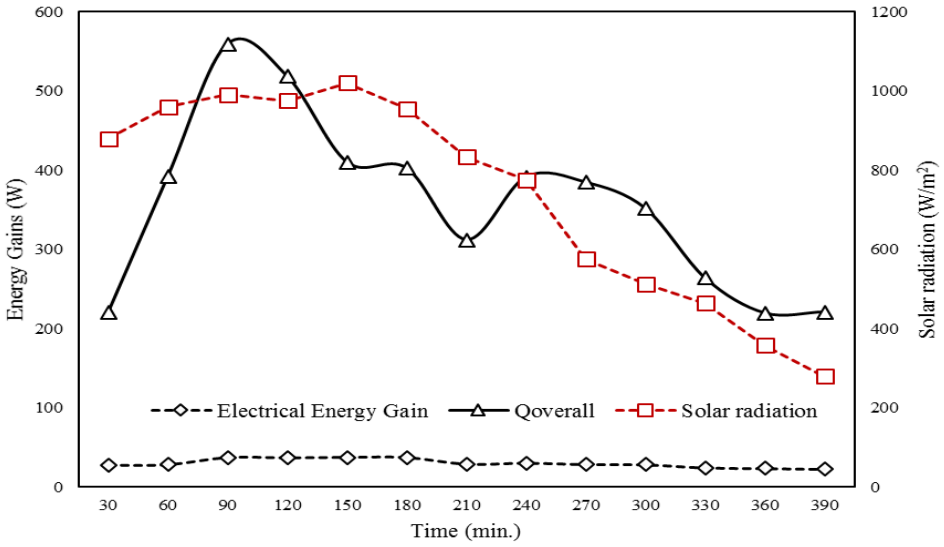

Figure 5.8. The change in energy gain and solar radiation over time.

5.2.6. Thermal Efficiency

It has been shown on Figure 5.9; the thermal efficiency of the system is decreasing. The decrease in the sunlight is not affecting the thermal efficiency of the system. According to the estimate by equation (4.12). The amount of solar radiation increased and the temperature of the water entering the model also increased.

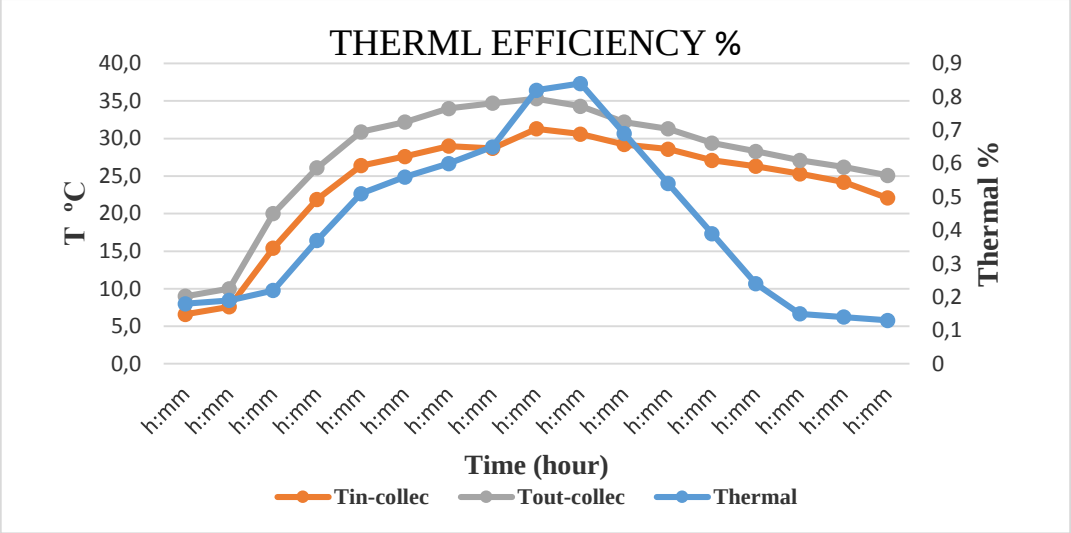

Figure 5.9. Thermal efficiency.

From Table 5.2 when Solar radiation is around 702 W/m^2, the temperature is 14.8°C. The average for PV model temperature inlet and outlet without fluid is also 8.44ºC. PV module efficiency with cooling is 18% and without cooling is 11%. Total thermal efficiency is 56%. The overall thermal and electrical gain is 78.2 W. In addiation, the average temperature for SC inlet and outlet without fluid is 3.66ºC and the efficiency for SC with cooling is 38%.

Table 5.2. Cooling with white spirit results analysis.

PVT module and solar collector process		Units
Average	ambient air temperature (ºC)	14.8 ºC
	Radiation W/m^2	600 W/m^2
	temperature for PV module inlet (ºC)	17.8 ºC
	temperature for PV module output (ºC)	26.24 ºC
	temperature for SC inlet (ºC)	25.34 ºC
	temperature for SC output (ºC)	29 ºC
	temperature for HE inlet (ºC)	10.6 ºC
	temperature for HE output (ºC)	25.36 ºC
	PV Actual power P = IV (W)	28.65 W
	PV Design power E (W)	28.65 W
	efficiency for PV module with cooling (%)	0.38%
	efficiency for PV module without cooling (%)	11%
	efficiency for SC with cooling (%)	022%
	system total thermal efficiency (%)	0.21%
	SC energy gain (W)	0.40W
	PV thermal energy gain (W)	0.58W
	total thermal energy gain (W)	0.43W
	system overall thermal and electrical gain (W)	78.2 W
	system overall thermal & electrical efficiency (%)	16%

In this table; SC: solar air collector, HE: Heat exchanger, PV: Photovoltaic system

The PV module temperature increased, as the solar radiation increased. When the solar radiation decreases, the electrical efficiency increases. At the same time, the temperature of the unit decreases. However, if solar radiation decreases at afternoon, the module outlet also decreases. The temperature unit varies according to the solar radiation and the White Spirit's fluids temperature changes at every time. The results showed that the efficiency of the unit with cooling is 3% which is higher than that of without cooling. The cooling process increases the volume of airflow using a cooling fan and increases power which resulted with the White Spirit's fluids temperature increases. Increases at cooling is affecting the average thermal efficiency of the entire system.

5.3. THE PHOTOVOLTAIC SYSTEM COOLING BY WATER WITH THERMAL ENERGY STORAGE

5.3.1. Solar Radiation and Ambient Air Temperature Differences

This test carried out on 16 December 2017, from 9:00 to 17:00. According to figure.5.10, the solar radiation varies between zero - 800 W/m^2, output power have been affected by these variations for radiation. At the start of the test, the radiation is 180W/m^2 at 10Am but it reaches the maximum value at 12:30 pm, which is 800 W/m^2. It then brought back to the lowest value at 17:00.

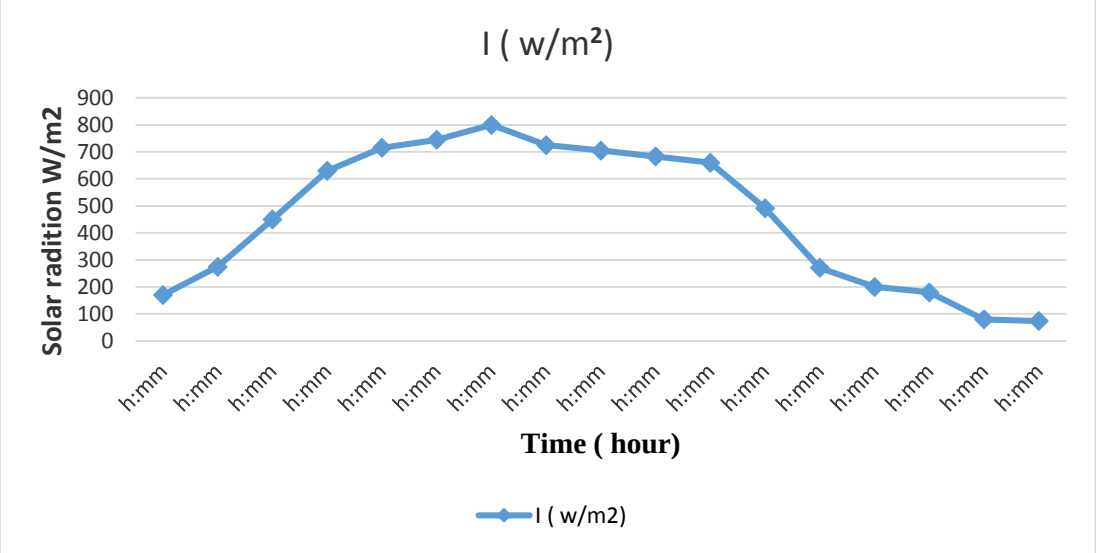

Figure 5.10. The variation in concentrated solar radiation.

Figure.5.11, has shown the relationship between It & Ta, when the It was 750 W/m^{2}max., the Ta = 10ºC, and when It was 620 W/m^2, then Ta = 14.5C max.

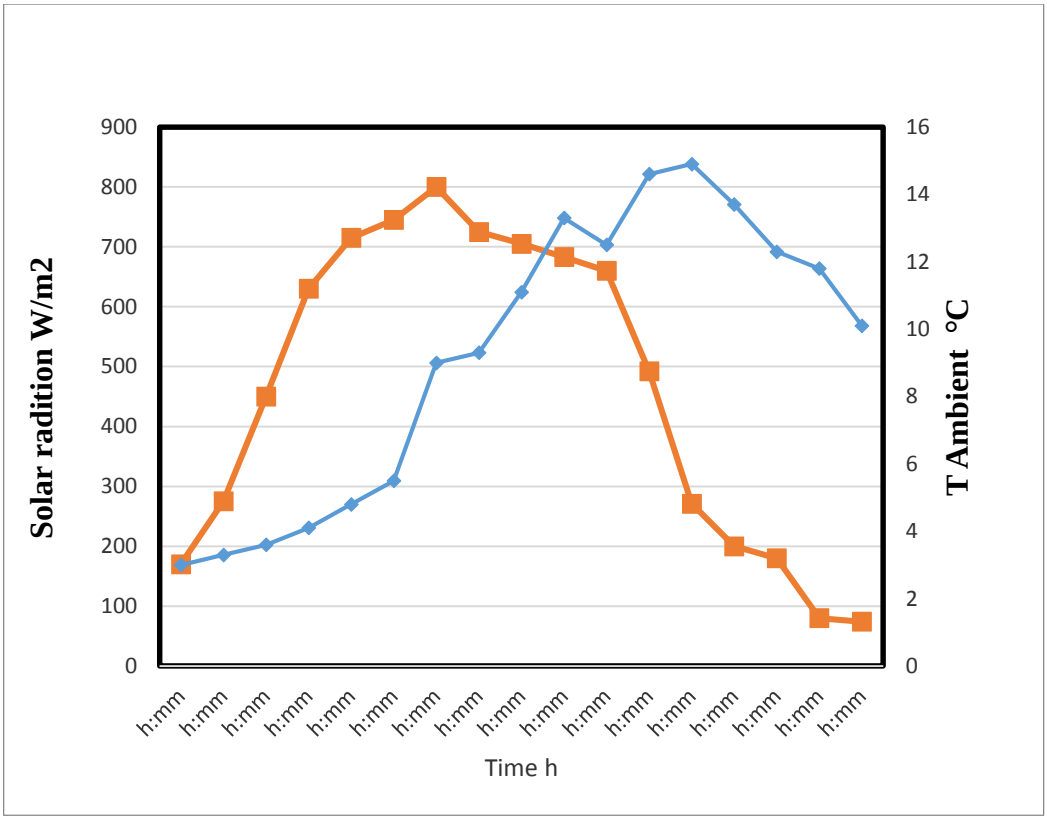

Figure 5.11. the relationship between It & Ta.

5.3.2. Electrical Energy

Electrical energy obtained in the gain modules PV module were calculated by using Eq. (4.11) and given in Figure 5.1.2 The radiation value is max 800 W/m^2 and min is 100 w/m^2 and the average is 450w/m^2, while the max. Et is 100W and the minimum is (12W) with average value 45W as seen in figure. 5.1.2. The radiation can be seen as above 800 W/m^2. This will increase the thermal efficiency. but the cooling system will decrease, and the cooling system composes of water pass through pipes will be fixed in the back of PV modules, the water then have to be cooled with air fan.

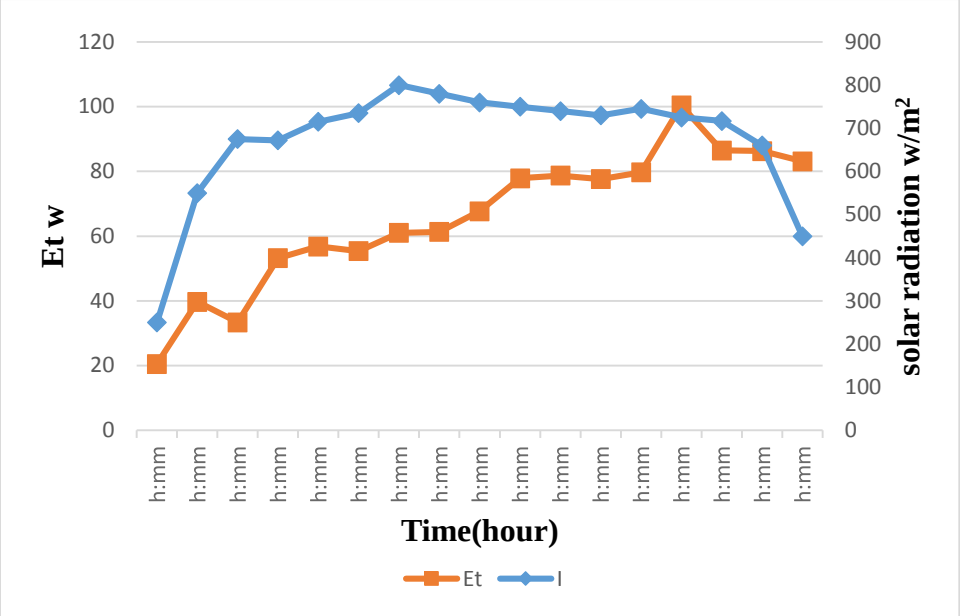

Figure 5.12. Electrical energy.

5.3.3. Actual Power

From figure 5.13, the solar radiation is above 700W/m^2. The output power is 35W, but while it is 400 W/m^2, more power have to be added to battery bank as nearly as 40 W. The power can be calculated by Eq. (4.10) resulted by the large amount of heat transfer from high solar radiation which is causing power losses.

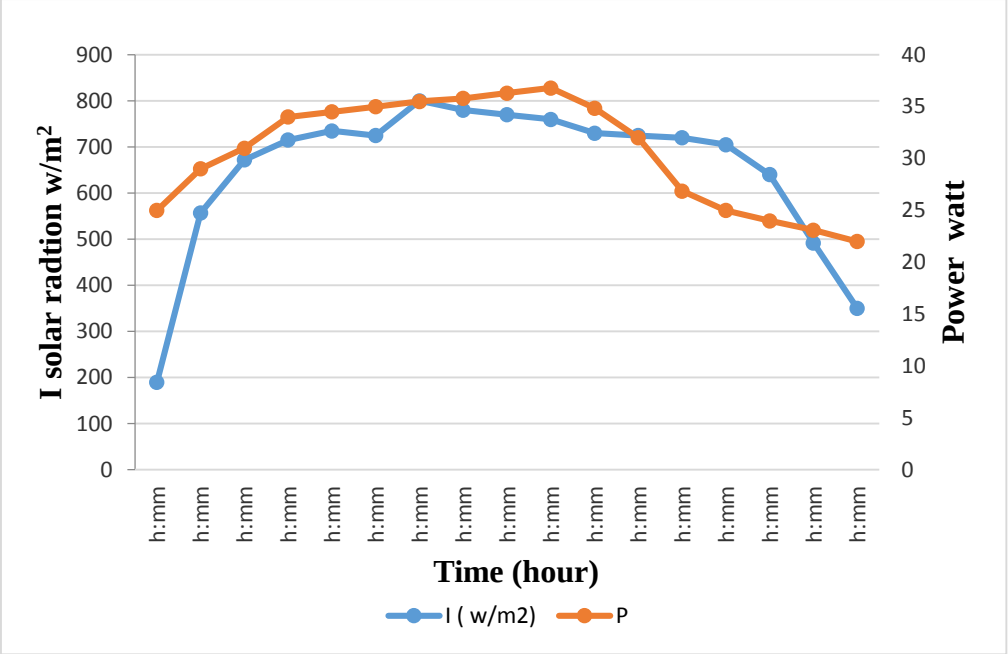

Figure 5.13. Solar radiation – Power Curve.

5.3.4. Efficiency

From figure 5.14, and Eq (4.4) the efficiency increased from 14 to 20 % during test period, also the range of Solar radiation is obsered as semi equal from 11:00 to 16:00. Therefore, the efficiency is not changing between 17-20 % during this period.

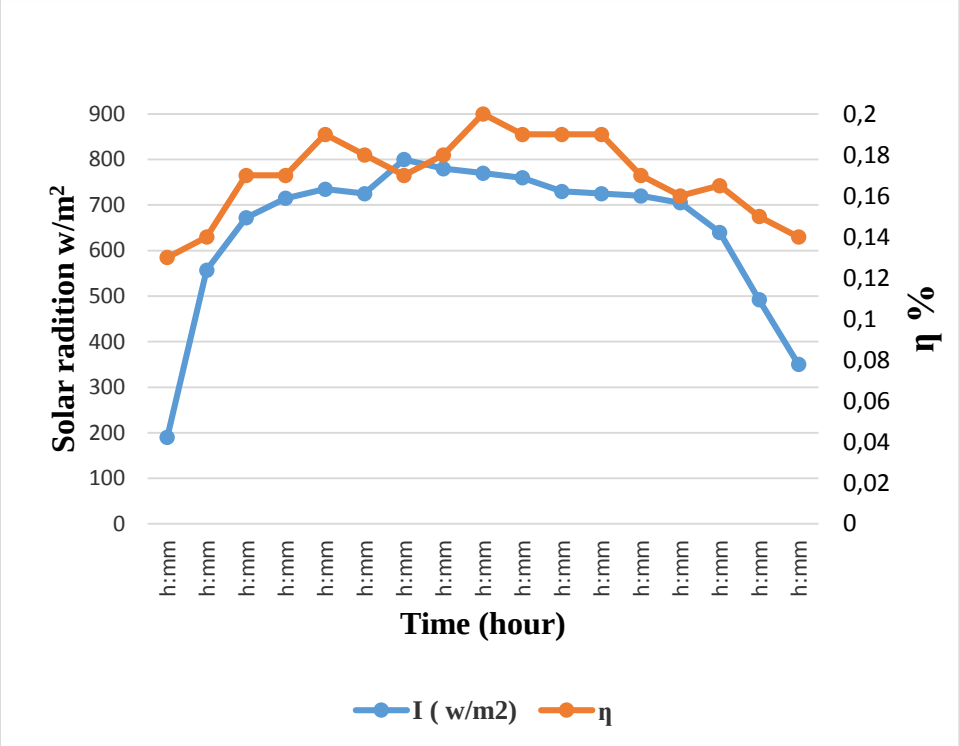

Figure 5.14. Solar radiation – Efficiency.

5.3.5. Thermal Energy Gains

In equation (4.13) and Fig 5.15, the thermal energy obtain in the model were calculated depending on the solar radiation, and the obtained thermal energy varies with a decrease in the radiation value. The electrical efficiency of the unit was not directly affected by this change; however, it reduced the power of the unit. As the radiation decreased, the collector that made up the system also decreased, and the unit thermal energy gained this quantity.

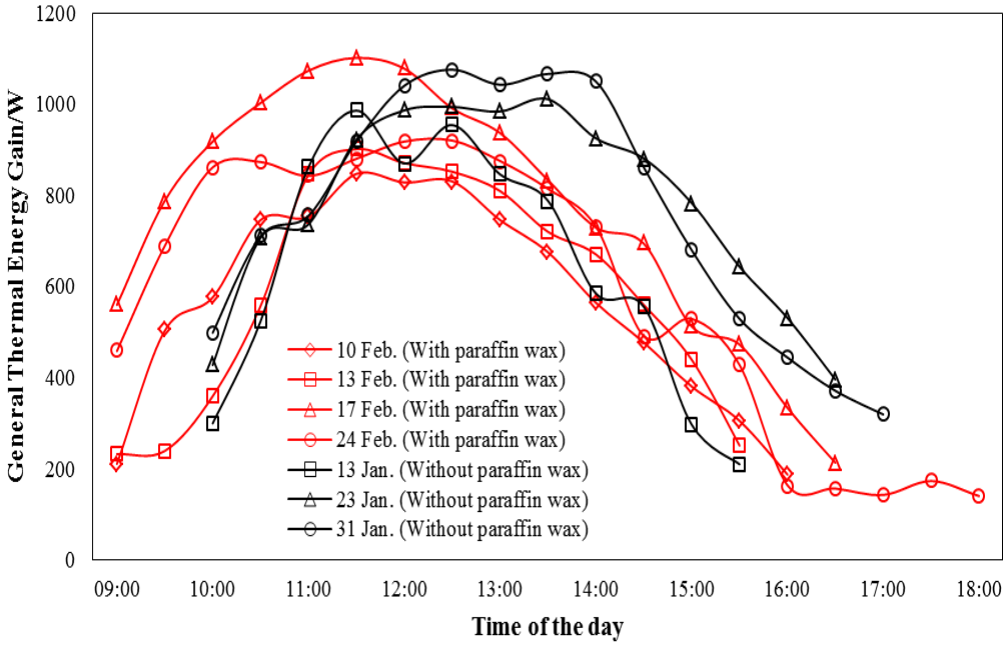

Figure 5.15. Solar Radiation& Thermal energy gains.

5.3.6. Thermal Efficiency

It has shown from Figure 5.16., that the thermal efficiency of the system decreases. That is the decrease in sunlight which is not affecting the thermal efficiency of the system. And by using equation (4.12), heat storage with paraffin wax can be calculated and it is affected by the decrease in solar radiation

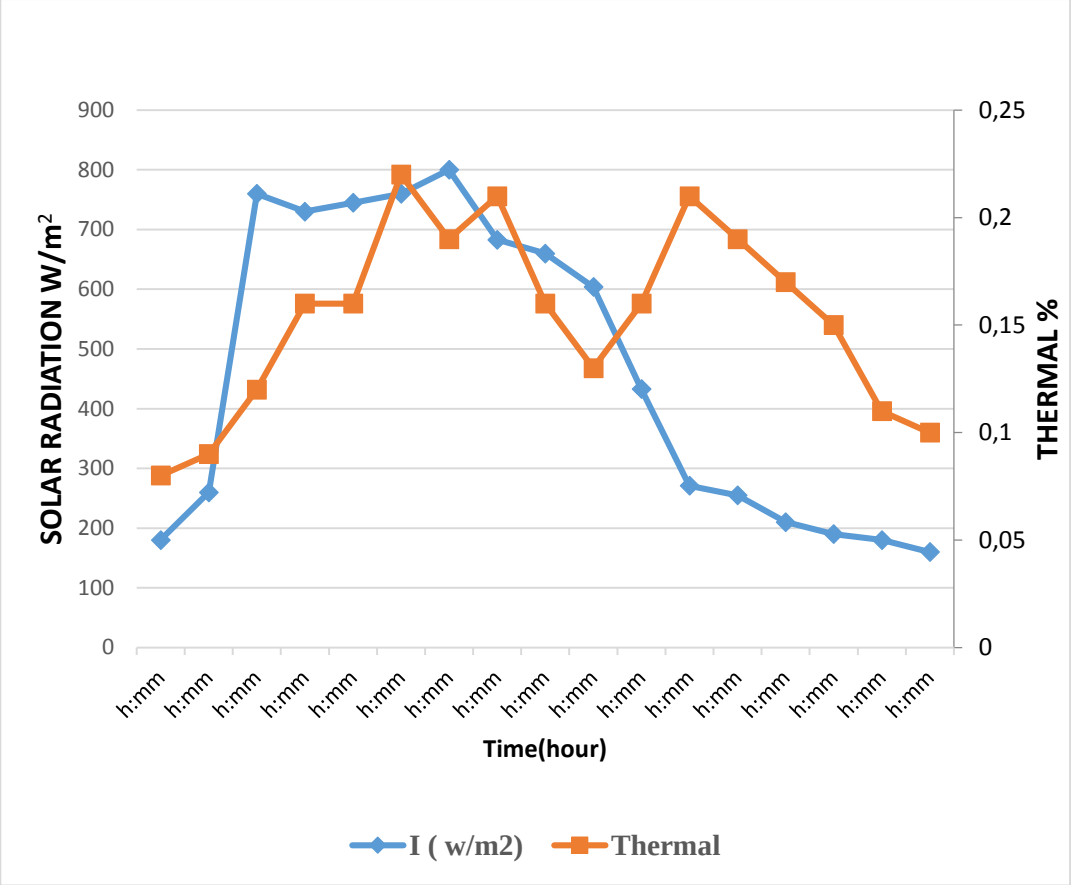

Figure 5.16. Solar radiation & thermal.

From Table 5.3., the solar radiation is 600 W/m2, the ambient air temperature is 10°C. The PV module temperature value is an average value changing between inlet and output which is 16.3 °C. The average temperature for solar collector between inlet and output is 20.45°and the efficiency of system ηt is 21.6%.

Table 5.3. Water cooling system results.

PVT module and solar collector process		Desecrip
Average	ambient temperature (◦C)	10°C
	Solar radiation W/m^2	600W/m^2
	temperature for PV module inlet (◦C)	13.6ºC
	temperature for PV module output (◦C)	19.7ºC
	temperature for Solar Colector inlet (◦C)	19.5ºC
	temperature for Solar Colector output (◦C)	21.4ºC
	PV Actual power P = IV (W)	25
	PV thermal energy gain Qpv , (W)	0.81
	Solar collector energy gain Qsc (W)	0.82
	total thermal energy gain Qtotal (W)	0.72
	efficiency for SC with cooling η_{sc} (%)	0.16
	solar panel energy E_t (W)	9.2
	solar colector energy E_t (W)	42
	system overall thermal & electrical gain Q_{overal}, (W)	177
	system overal thermal efficiency η_{overal} (%)	41
	efficiency for PV module with cooling η_{pv} (%)	0.21%
	Energy Et (W)	51.2
	Thermal efficiency (%)	14

The evaluation made in this section can be summarized as follows. The average temperature of the solar panels between the entry and exit of water is 16.3 °C and it is considered with a slight difference. Electrical efficiency increased when the solar radiation decreased. At this unit time, temperature has also decreased. Increasing water flow inside the pipes in the backwards of the solar module contributes to increasing the efficiency of the unit. The changes that occur in the current and the voltage contribute to increasing the electrical power.

5.4. COOLING WITH ETHYL ALCOHOL

5.4.1. Solar Radiation Curve

According to Figure 5.17, three hours test, 30 minutes' interval, the solar radiation varies between 320 and 980 W/m^2. The maximum value was observed after 14:00 hour which was (940W/m^2). It is close to full sun value as standard value 1000W/m^2, while the average is 564W/m^2. It is evident from the figure that the solar radiation is less than 500W/m^2 according to 45% of samples. This range produces nearly 50% of maximum current of PV module at 25^{o}C.

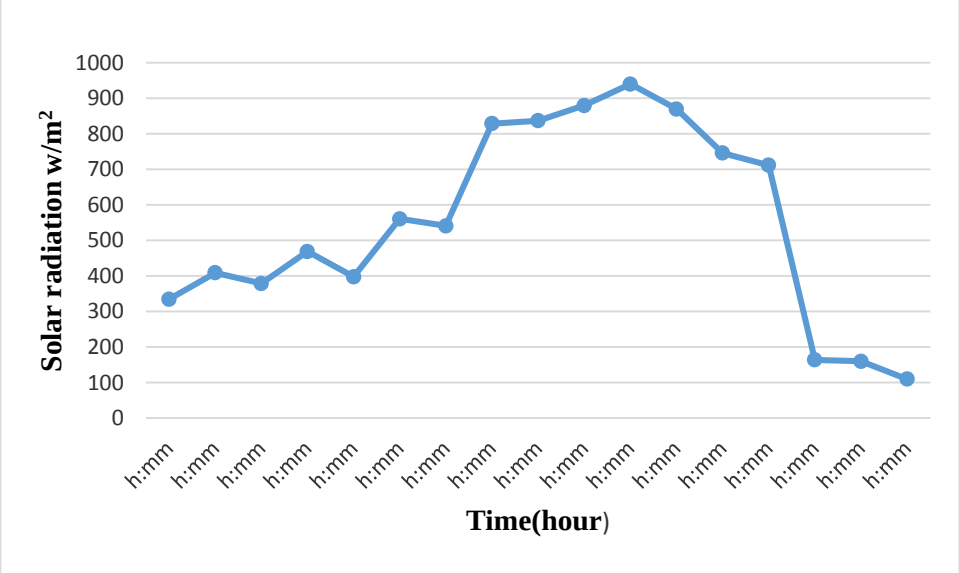

Figure 5.17. The variation in concentrated solar radiation.

5.4.2. Curve Solar Radiation and Ambient Air Temperature

Figure 5.18 in which noted the ambient air temperature continues to increase until reaching the max. temperature value 40^{o}C after 14:00 hour since the test beginning, then it has to be continued to decrease the 35^{o}C at the end of test.

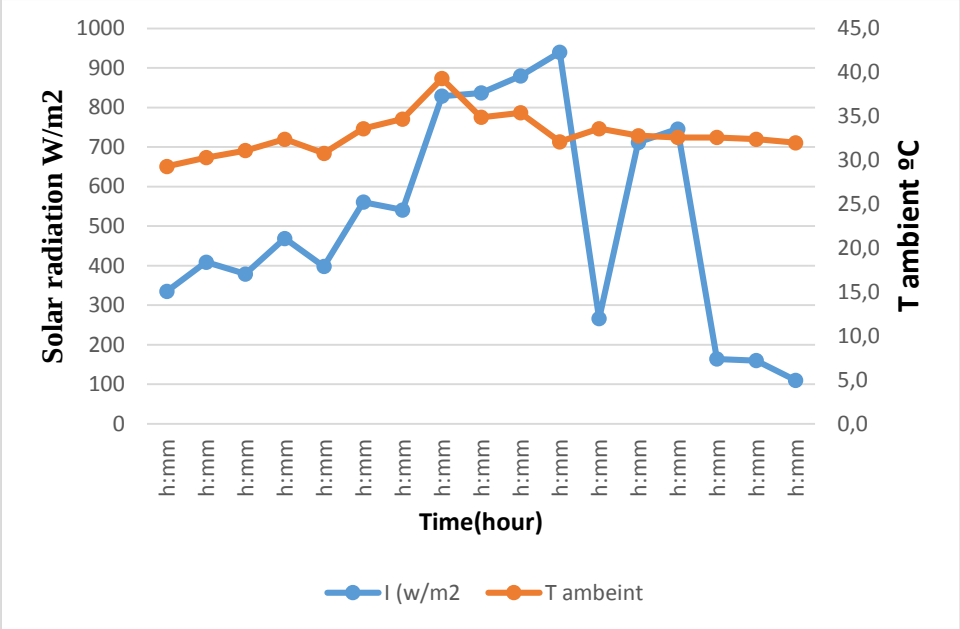

Figure 5.18. Solar radiation – T ambient.

5.4.3. PV Module Voltage – Current Curve

Solar radiation evolution and unit current has been shown in Fig.5.19. Unit current changes is depending on solar radiation. From notes of Figure 5.19, the current ranger between can be determined as 0.6-1.62A with average 1A and the voltage range is between 17.1 to 19V with average 18V value, the voltage samples is above 17V, while current is under 1A during the first 50 minutes then after its range is between 1 to 1.62A on the rest of test. The max. value of current was recorded after about two hours (130 minutes) of test which was 1.62 A due to 940 W/m^2 solar radiation.

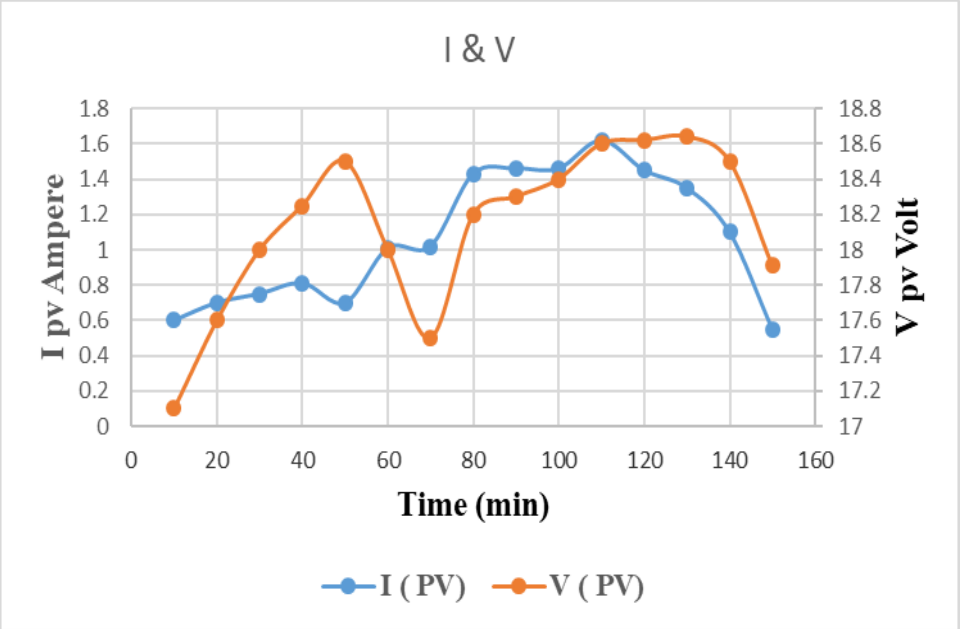

Figure 5.19. PV module V & I.

5.4.4. Solar Radiation– Module Efficiency

Figure. 5.20 has shown the solar radiation module efficiency curve. The efficiency which is between 0.05 to 18%, is semi constant from 09:00 to 14:00 hour. The Solar radiation at the same period is ranged from 300 to 900 W/m^2. The solar module efficiency value increases to 18%, when the solar radiation intensity is close to 600W/m^2. When solar radiation limit is above this value, then the efficiency is just 12%. The module efficiency can be calculated as Eq. (4.4).

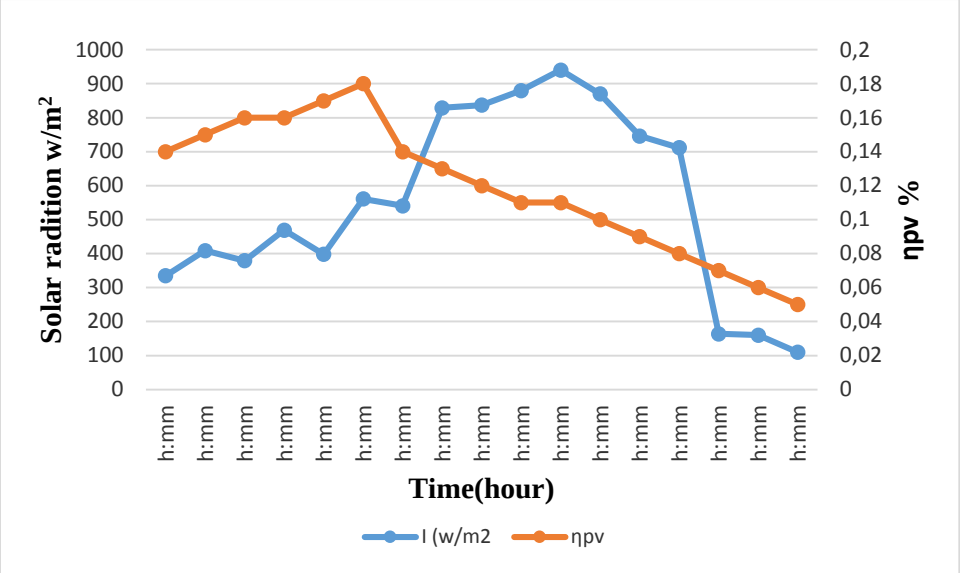

Figure 5.20. Solar radiation & module efficiency.

5.4.5. Solar Radiation - Total Efficiency

Figure.5.21, has shown that the max. reading value, which is 19.54%. While the minimum value is 5.8 %, then the average is 21.4 %. The lower value is observed after 110 min., with ranges between 5.8-14.65%. This situation for alcohol fluid coolant as the solar radiation on this period is high can be explained by Eq. (4.6): It is estimating total efficiency.

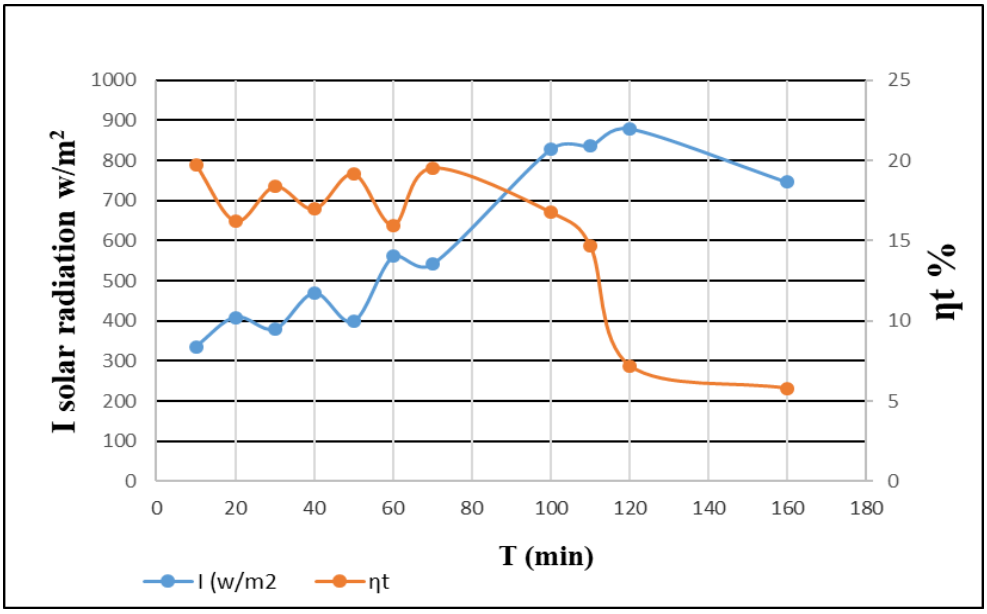

Figure 5.21. Solar radiation & Total efficiency.

5.4.6. Solar Radiation - Overall Thermal & Electrical Gain

The change in the overall thermal efficiency and solar radiation over time are given in Figure 5.22. The average overall thermal efficiency of the CPV/T is calculated as 53%. Also, the efficiency by Eq. (4.6) can be calculated.

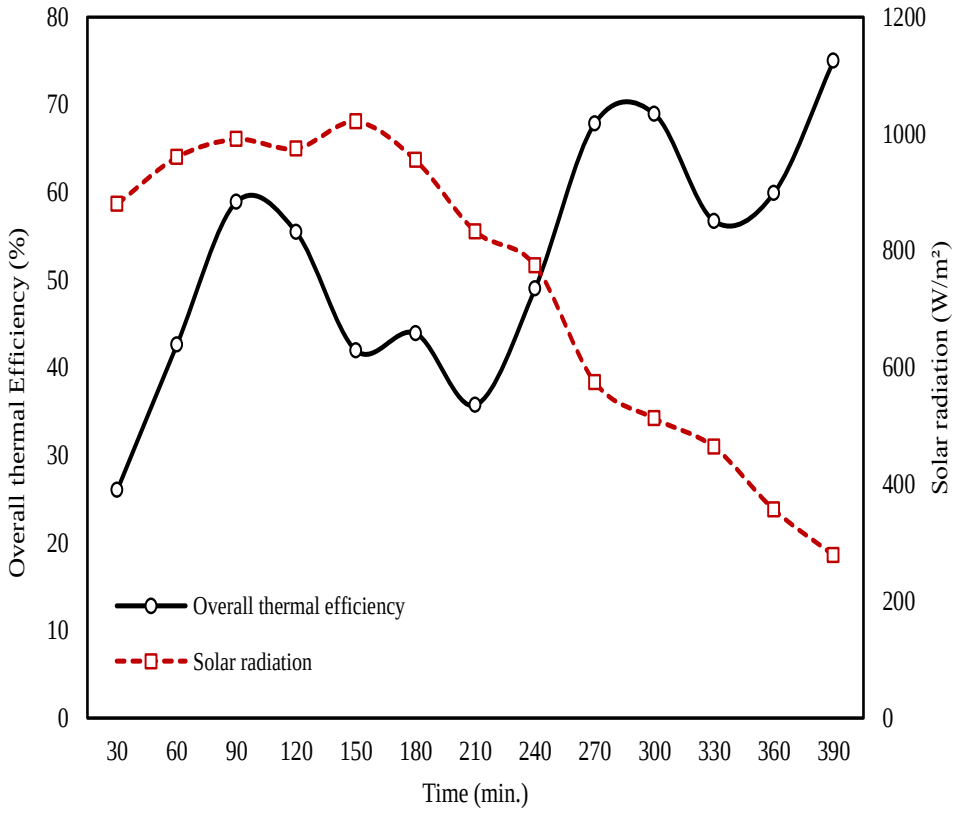

Figure 5.22. Solar radiation & overall thermal efficiency.

From table 5.4, The Solar radiation is 564 W/m^2 and the ambient air temperature is 33°C. The temperature of PV module is changing between inlet and output which has an average value as 0.2^{o}C. The average temperature for solar collector between inlet and output is 2.3°C and the efficiency of system is 13%.

Table 5.4. Cooling with ethyl alcohol results.

PVT module and solar collector process		Descrbe.
Average	ambient air temperature (◦C)	33 C
	Solar Radiation W/m^2	600 W/m^2
	temperature for PV module inlet (◦C)	35 C
	temperature for PV module output (◦C)	35.2 C
	temperature for Solar Colector inlet (◦C)	35.4 C
	temperature for Solar Colector output (◦C)	37.7 C
	temperature for HE inlet (◦C)	13.3 C
	temperature for HE output (◦C)	C
	PV Actual power P = IV (W)	19.33 W
	PV Desighn power E (W)	28.65 W
	PV thermal energy gain Qpv , (W)	0.60
	Solar collector energy gain Qsc (W)	0.72
	total thermal energy gain Qtotal (W)	0.86
	efficiency for PV module with cooling η_{pv} (%)	0.23
	efficiency for SC with cooling η_{sc} (%)	0.19
	solar panel energy E_{PV}(W)	19.3
	solar colector energy E_{SC} (W)	1.95
	system overall thermal & electrical gain Q_{overal}, (W)	60
Total	Total efficiency of system η_t	0.16
	Total Energy Et (W)	21.4

The research made in this section can be concluded as follows: “the higher the solar radiation, the lower the unit temperature in this system”. The model efficiency at cooling was 23% higher than that of cooling. As the solar radiation increases, the model is cooled through the inlet and outlet of the ethyl alcohol. Thus, the electrical

efficiency has increased. Moreover, when the solar radiation is decreased, the unit temperature is also decreased at the same time, so the efficiency is beginning to be higher. However, the unit outlet energy is reduced due to lower solar radiation. The alcohol temperature inside the solar collector increases simultaneously with increasing in solar radiation. PV models has not been completely cooled by the system due to the efficiency reduction with the difference between the input temperatures.

Table 5.5. Different Cooling systems performance analysis.

Description	Water	Spirit	Ethyl Alcohol
Average ambient air temperature (◦C)	10	14.8	33
Average Radiation W/m^2	600	600	600
Average temperature for PV module inlet (◦C)	13.6	17.8	35
Average temperature for PV module output (◦C)	19.7	26.24	35.2
Ave. temperature for Solar Collector inlet (◦C)	19.5	25.34	35.4
Ave. temperature for Solar Collector output (◦C)	21.4	29	37.7
Average PV Actual power (W)	25	10.6	19.3
Average PV thermal energy gain Qpv , (W)	0.81	0.58	0.60
Average Solar collector energy gain Qsc (W)	0.82	0.40	0.72
Average total thermal energy gain Qtotal (W)	0.72	0.43	0.86
Average efficiency for SC η_{sc} (%)	0.16	0.22	0.19
Average efficiency for PV module η_{pv} (%)	0.21	0.38	0.23
Total efficiency of system η_t	0.56	0.21	0.16
Average solar panel energy E_{PV} (W)	9.5	28.67	19.3
Average solar collector energy E_{SC} (W)	42	27.4	19.6
Total Energy (W) Et	51.5	28.65	21.3
Average system overall thermal & electrical gain,(W)	177	78	60
Ave. system overall thermal efficiency $\eta_{overall}$ (%)	41	16	59.89
Thermal efficiency (%)	14	38	15

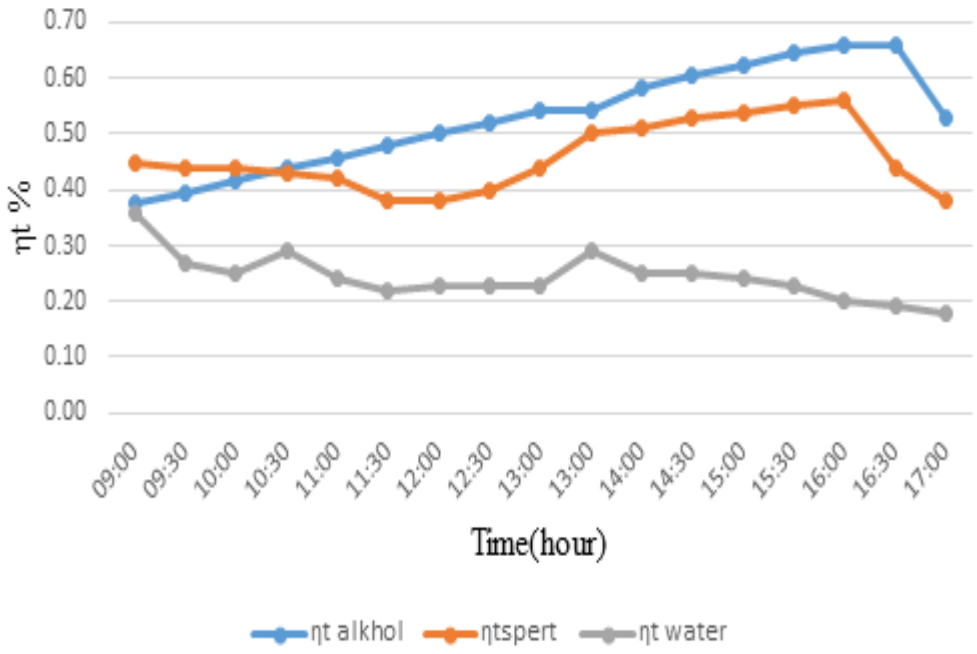

Figure 5.22. Total efficiency of the three cooling.

CHAPTER 6

CONCLUSION AND RECOMMENDATION

6.1. CONCLUSION

The Experiment Model was designed in Energy Labs at the Energy System Department in Karabük University. The model specially designed to use two circuits for cooling the fluid circuit and the air circuit with the decreasing the temperature of solar panels. That accomplish this study well. A type of heat exchanger is added to connect the two circles and retort tubes installed behind the solar panels. This setting is manufactured and assembled to measure the performance parameters required for both the PVT collector (with different coolers) and the PV panel (reference). The variables can be listed as temperature, Solar radiation, voltage, coolant flow rate, current, etc.

In water experiments, the following results can be concluded:

The average daily low PV surface temperature raises with rising coolant flow rate. At the case of a 0.5 L/ min flow rate, the average daily decrease in PV roof temperature was around 10°C.

In this study, all results changes between the three fluids are studied. These are;

- Average Efficiency PV Unit ηpv (18%) – the Spirit.
- The overall efficiency of the system- the Spirit 56%.
- Average solar collector energy Esc (27.4W) - the spirit.
- Total Energy (51.5W) - water.

- Average system overall thermal & electrical gain $O_{overall}$, (177W) - water.
- Average system overall thermal efficiency η_{overal} (59.89%) - ethyl alcohol.
- Thermal efficiency (38%) - the spirit.

6.2. RECOMMENDATIONS

Our recommendations in this study are as follows:

- Increasing the fluid's circle length is more effective for cooling, because increasing the distance causes the liquid to cool.
- This new model opens new horizons for important issues for researchers in the field of refrigeration around the world.
- Water-cooling is a simple, safe, effective, and available method for non-specialists.
- Household water can be used to cool PV system, where water is utilized twice. The first is in the photovoltaic system and the second is in domestic services as irrigation, washing machine, car washing and cleaning of floor surfaces.
- Currently, other coolers, such as spirit and alcohol are only restricted to educational purposes.
- Take advantage of the air circuit in the complex for the drying process.
- Try with other fluids such as the Nano-fluid.

REFERENCES

1. Bahaidarah, H., Subhan, A., Gandhidasan, P. & Rehman, S. Performance evaluation of a PV (photovoltaic) module by back surface water cooling for hot climatic conditions. ***Energy*** **59**, 445–453 (2013).

2. Teo, H. G., Lee, P. S. & Hawlader, M. N. A. An active cooling system for photovoltaic modules. *Appl.* ***Energy*** **90**, 309–315 (2012).

3. Chandrasekar, M., Suresh, S., Senthilkumar, T. & Ganesh Karthikeyan, M. Passive cooling of standalone flat PV module with cotton wick structures. ***Energy Convers. Manag.*** **71**, 43–50 (2013).

4. Valeh-E-Sheyda, P., Rahimi, M., Karimi, E. & Asadi, M. Application of two-phase flow for cooling of hybrid microchannel PV cells: A comparative study. ***Energy Convers. Manag.*** **69**, 122–130 (2013).

5. Moharram, K. A., Abd-Elhady, M. S., Kandil, H. A. & El-Sherif, H. Enhancing the performance of photovoltaic panels by water cooling. ***Ain Shams Eng***. *J.* **4**, 869–877 (2013).

6. 21.pdf.

7. Mahalingam, S. & Sharan, A. M. Optimal Balancing of the Robotic Manipulators. 828–835 (1986) doi:10.1109/**robot.**1986.1087570.

8. Gee, J. M. & Hansen, B. R. Photovoltaic concentrator cell measurement methods. ***Sol. Cells*** **18**, 281–288 (1986).

9. Salim, A. A. & Eugenio, N. N. A comprehensive report on the performance of the longest operating 350 kW concentrator photovoltaic power system. ***Sol. Cells*** **29**, 1–24 (1990).

10. Hein, S. *et al.* Progression from compensated hypertrophy to failure in the pressure-overloaded human: Heart structural deterioration and compensatory mechanisms. ***Circulation*** **107**, 984–991 (2003).

11. Bhatnagar, M. C. & Joshi, J. C. Field performance of concentrated photovoltaic modules. ***Sol. Cells*** **28**, 343–350 (1990).

12. Royne, A., Dey, C. J. & Mills, D. R. Cooling of photovoltaic cells under concentrated illumination: A critical review. *Sol. Energy Mater.* ***Sol. Cells*** **86**, 451–483 (2005).

13. Coventry, J. S., Franklin, E. & Blakers, A. Thermal and electrical performance of a concentrating PV / Thermal collector : results from the ANU CHAPS collector. ***ANU Res****. Publ.* 1–6 (2002).

14. Chemisana, D., Ibáñez, M. & Rosell, J. I. Characterization of a photovoltaic-thermal module for Fresnel linear concentrator. ***Energy Convers. Manag***. **52**, 3234–3240 (2011).

15. Kribus, A. *et al.* A miniature concentrating photovoltaic and thermal system. ***Energy Convers. Manag***. **47**, 3582–3590 (2006).

16. Vorobiev, Y., González-Hernández, J., Vorobiev, P. & Bulat, L. Thermal-photovoltaic solar hybrid system for efficient solar energy conversion. ***Sol. Energy*** **80**, 170–176 (2006).

17. Mittelman, G., Kribus, A. & Dayan, A. Solar cooling with concentrating photovoltaic/thermal (CPVT) systems. ***Energy Convers. Manag***. **48**, 2481–2490 (2007).

18. Bohman, H. & Nilsson, D. Market overlap and the direction of exports: A new approach of assessing the Linder hypothesis. ***CESIS—Electronic Work***. *Pap. Ser. Pap.* (2007).

19. Sangani, C. S. & Solanki, C. S. Experimental evaluation of V-trough (2 suns) PV concentrator system using commercial PV modules. ***Sol. Energy Mater***. *Sol. Cells* **91**, 453–459 (2007).

20. Mokri, A. & Emziane, M. Concentrator Photovoltaic Technologies and Market: A Critical Review. *Proc.* ***World Renew. Energy Congr***. *– Sweden, 8–13 May, 2011, Linköping, Sweden* **57**, 2738–2742 (2011).

21. Manokar, A. M., Winston, D. P. & Vimala, M. Performance Analysis of Parabolic trough Concentrating Photovoltaic Thermal System. ***Procedia Technol***. **24**, 485–491 (2016).

22. Garg, H. P. & Adhikari, R. S. Conventional hybrid photovoltaic/thermal (PV/T) air heating collectors: Steady-state simulation. *Renew*. ***Energy*** **11**, 363–385 (1997).

23. Ceballos, S. M. Concentrated photovoltaic **energy**. (2015).

24. Al-Alili, A., Hwang, Y., Radermacher, R. & Kubo, I. A high efficiency solar air conditioner using concentrating photovoltaic/thermal collectors. ***Appl. Energy*** **93**, 138–147 (2012).

25. Arshad, R., Tariq, S., Niaz, M. U. & Jamil, M. Improvement in solar panel efficiency using solar concentration by simple mirrors and by cooling. *2014 Int.*

***Conf. Robot. Emerg. Allied Technol. Eng. iCREATE** 2014 - Proc.* 292–295 (2014) doi:10.1109/iCREATE.2014.6828382.

26. Sachdeva, R. & Kakkar, S. A Novel Approach in Cloud Computing for Load Balancing Using Composite Algorithms. ***Int. J. Adv. Res. Comput. Sci. Softw. Eng***. **7**, 51–56 (2017).

27. Sopian, K., Yigit, K. S., Liu, H. T. & Veziroglu, T. N. Performance Analysis of Photovoltaic. ***Energy Convers. Manag.*** **37**, 1657–1670 (1996).

28. Bai, Y. *et al*. Experimental and numerical study of a directly PV-assisted domestic hot water system. ***Sol. Energy*** **85**, 1979–1991 (2011).

29. Jarimi, H., Abu Bakar, M. N., Othman, M. & Din, M. H. Bi-fluid photovoltaic/thermal (PV/T) solar collector: Experimental validation of a 2-D theoretical model. ***Renew. Energy*** **85**, 1052–1067 (2016).

30. Royne, A. & Dey, C. J. Design of a jet impingement cooling device for densely packed PV cells under high concentration. ***Sol. Energy*** **81**, 1014–1024 (2007).

31. Slimani, M. E. A., Amirat, M. & Bahria, S. Analysis of thermal and electrical performance of a solar PV/T air collector: Energetic study for two configurations. ***3rd Int. Conf. Control. Eng. Inf. Technol. CEIT*** *2015* 8–10 (2015) doi:10.1109/CEIT.2015.7232999.

32. Sami, S. Modeling and Simulation of a Novel Combined Solar Photovoltaic-Thermal Panel and Heat Pump Hybrid System. ***Clean Technol***. **1**, 89–113 (2018).

33. Veramendi, J. People on love drug **MDMA** still know who to trust. 1–5 (2020).

34. Kaldellis, J. & Zafirakis, D. Experimental investigation of the optimum photovoltaic panels' tilt angle during the summer period. ***Energy*** **38**, 305–314 (2012).

35. 15.pdf.

36. Mehleri, E. D., Zervas, P. L., Sarimveis, H., Palyvos, J. A. & Markatos, N. C. Determination of the optimal tilt angle and orientation for solar photovoltaic arrays. ***Renew. Energy*** **35**, 2468–2475 (2010).

37. Mondol, J. D., Yohanis, Y. G. & Norton, B. The impact of array inclination and orientation on the performance of a grid-connected photovoltaic system. ***Renew. Energy*** **32**, 118–140 (2007).

38. Abdolzadeh, M. & Ameri, M. Improving the effectiveness of a photovoltaic water pumping system by spraying water over the front of photovoltaic cells. ***Renew.***

Energy **34**, 91–96 (2009).

39. Slimani, M. E. A., Amirat, M. & Bahria, S. Analysis of thermal and electrical performance of a solar PV/T air collector: Energetic study for two configurations. ***3rd Int. Conf. Control. Eng. Inf. Technol. CEIT*** *2015* 1–6 (2015) doi:10.1109/CEIT.2015.7232999.

40. Zondag, H. A., De Vries, D. W., Van Helden, W. G. J., Van Zolingen, R. J. C. & Van Steenhoven, A. A. The thermal and electrical yield of a PV-thermal collector. ***Sol. Energy*** **72**, 113–128 (2002).

41. Martin, O. L. E. Pergamon 0038-092X(95)00072-**O**. **55**, 453–462 (1995).

42. Fujisawa, T. & Tani, T. Annual exergy evaluation on photovoltaic-thermal hybrid collector. ***Sol. Energy Mater. Sol. Cells*** **47**, 135–148 (1997).

43. Harbi, Y. A. L., Eugenio, N. N. & Zahrani, S. A. L. **RENEWABLE ENERGY**. **5**, 5–8 (1998).

44. Tripanagnostopoulos, Y., Nousia, T. H., Souliotis, M. & Yianoulis, P. HYBRID PHOTOVOLTAIC / **THERMAL SOLAR SYSTEMS**. **72**, 217–234 (2002).

45. Zondag, H. A. Flat-plate PV-Thermal collectors and systems: A review. *Renew. Sustain.* ***Energy Rev***. **12**, 891–959 (2008).

46. Popovici, G., Valeriu, S., Dorin, T. & Chereche, N.-C. Efficiency improvement of photovoltaic panels by using air cooled **heat sinks**. **85**, 425–432 (2016).

47. Srivastava, A. *et al*. Laparoscopic radical nephrectomy: A journey from T1 to very large T2 tumors. ***Urol. Int.*** **82**, 330–334 (2009).

48. Ahmad, A., Mushrifah, I. & Lim, E. C. Seasonal Influence on Water Quality and Heavy Metals Concentration in Tasik Chini , **Peninsular Malaysia**. 300–303 (2008).

49. Hosn, R. A. (12) United States Patent (10) **Patent No** .: **2**, (2009).

50. Touafek, K., Haddadi, M. & Malek, A. Design and modeling of a photovoltaic thermal collector for domestic air heating and electricity production. ***Energy Build.*** **59**, 21–28 (2013).

51. Moradi, K., Ali Ebadian, M. & Lin, C. X. A review of PV/T technologies: Effects of control parameters. ***Int. J. Heat Mass Transf***. **64**, 483–500 (2013).

52. Tonui, J. K. & Tripanagnostopoulos, Y. Performance improvement of PV/T solar collectors with natural air flow operation. ***Sol. Energy*** **82**, 1–12 (2008).

53. Kalogirou, S. A. Use of TRNSYS for modelling and simulation of a hybrid pv – thermal solar system **for Cyprus**. **23**, 247–260 (2001).

54. Wylie, B. K. & Homer, C. DigitalCommons @ University of Nebraska - Lincoln A Strategy for Estimating Tree Canopy Density **Using Landsat 7 ETM + and High Resolution Images Over Large Areas.** (2001).

55. Sandnes, B. & Rekstad, J. A Photovoltaic / Thermal (Pv / T) Collector With A Polymer Absorber Plate . Experimental Study And **Analytical Model**. **72**, 63–73 (2002).

56. Zondag, H. A., Vries, D. W. De, Helden, W. G. J. Van & Zolingen, R. J. C. Van. T he yield of different combined PV-**thermal collector designs**. **74**, 253–269 (2003).

57. Ahmad, N., Khandakar, A., El-tayeb, A., Benhmed, K. & Iqbal, A. Novel Design for Thermal Management of PV Cells in Harsh Environmental Conditions. (2018) **doi:**10.3390/en11113231.

58. Zhu, L., Boehm, R. F., Wang, Y., Halford, C. & Sun, Y. Solar Energy Materials & Solar Cells Water immersion cooling of PV cells in a high concentration system. ***Sol. Energy Mater.*** **95**, 538–545 (2011).

59. Diwania, S., Agrawal, S., Siddiqui, A. S. & Singh, S. Photovoltaic – thermal (PV / T) technology : a comprehensive review on applications and its advancement. ***Int. J. Energy Environ. Eng.*** (2019) doi:10.1007/s40095-019-00327-y.

60. Erdil, E., Ilkan, M. & Egelioglu, F. An experimental study on energy generation with a photovoltaic (PV)– **solar thermal hybrid system**. **33**, 1241–1245 (2008).

61. Tonui, J. K. & Tripanagnostopoulos, Y. Air-cooled PV/T solar collectors with low cost performance improvements. ***Sol. Energy*** **81**, 498–511 (2007).

62. Abu-rahmeh, T. M. Efficiency of Photovoltaic Modules Using Different Cooling Methods : A Comparative Study. 32–45 (2017) **doi:**10.4236/jpee.2017.59003.

63. Dubey, S. & Tiwari, G. N. Analysis of PV / T flat plate water collectors connected in series. ***Sol. Energy*** **83**, 1485–1498 (2009).

64. Heat, C. **CHAPTER** 2. 22–67.

65. Aboltins, A. & Machinery, A. Air Heated Solar Collectors And **Their Applicability**. (2012).

66. Leonforte, F. & Pero, C. Del. ScienceDirect Design , modeling and performance monitoring of a photovoltaic – **thermal (PVT) water collector**. **112**, 85–99 (2015).

67. Alami, A. H. Effects of evaporative cooling on efficiency of photovoltaic modules. ***Energy Convers. Manag***. **77**, 668–679 (2014).

68. Teo, H. G., Lee, P. S. & Hawlader, M. N. A. An active cooling system for photovoltaic modules. ***Appl. Energy*** **90**, 309–315 (2012).

69. Sahay, A., Sethi, V. K., Tiwari, A. C. & Pandey, M. A review of solar photovoltaic panel cooling systems with special reference to Ground coupled central panel cooling system (GC-CPCS). ***Renew. Sustain. Energy Rev***. **42**, 306–312 (2015).

70. Jagathdarani, C., Student, P. G., College, K. S. R., Glass, A. & Pv, G. Elevating the Efficiency of the Solar G2GPVT System by Inherent Cooling Method and Monitoring using LabVIEW. *2016 2nd Int. Conf. Adv. Electr. Electron. Information,* ***Commun. Bio-Informatics*** 525–529 (2016) doi:10.1109/AEEICB.2016.7538345.

71. Siecker, J. & Kusakana, K. Cooling Photovoltaic Technologies Systems : Survey Of.

72. Dubey, S. & Tiwari, G. N. Analysis of PV/T flat plate water collectors connected in series. ***Sol. Energy*** **83**, 1485–1498 (2009).

73. Sarhaddi, F., Farahat, S., Ajam, H., Behzadmehr, A. & Mahdavi Adeli, M. An improved thermal and electrical model for a solar photovoltaic thermal (PV/T) air collector. ***Appl. Energy*** **87**, 2328–2339 (2010).

74. Røyne, A. Cooling devices for densely packed, high concentration **PV arrays**. 135 (2005).

75. Shahsavar, A. & Ameri, M. Experimental investigation and modeling of a direct-coupled PV/T air collector. ***Sol. Energy*** **84**, 1938–1958 (2010).

76. Ceylan, İ. *et al.* A New Hybrid System Design for Thermal Energy Storage. ***J. Therm.*** *Sci.* **29**, 1300–1308 (2020).

77. Ceylan, I., Gürel, A. E., Demircan, H. & Aksu, B. Cooling of a photovoltaic module with temperature controlled solar collector. ***Energy Build***. **72**, 96–101 (2014).

78. Bai, Y. *et al.* Experimental and numerical study of a directly PV-assisted domestic hot water system. ***Sol. Energy*** **85**, 1979–1991 (2011).

79. Shahsavar, A. & Ameri, M. Experimental investigation and modeling of a direct-coupled PV/T air collector. ***Sol. Energy*** **84**, 1938–1958 (2010).

RESUME

ISMAIL ALBARKI. I completed primary and elementary education in Benghazi, the second city in Libya. In 1992, I graduated from Physics Department, Faculty of Sciences, Musrata University. After that, I worked as a Physical laboratory technician in the period 1994-2000. In the period 2000-2003, I got a scholarship to continue his MSc education in Malaysia in University Kebangsaan (UKM). Since 2004, he worked as lecturer in College of Electrical and Electronic Technology. Benghazi. In 2014, he got a scholarship to continue his PhD education in Turkey. He started his PhD academic program at Karabuk University at 2015-2016 autumn.